RSC Advances

Toward Point-of-Care Diagnostics with Consumer Electronic Devices: The Expanding Role of Nanoparticles

Journal:	*RSC Advances*
Manuscript ID:	RA-REV-11-2014-015036.R1
Article Type:	Review Article
Date Submitted by the Author:	11-Feb-2015
Complete List of Authors:	Petryayeva, Eleonora; University of British Columbia, Chemistry Algar, Walter; University of British Columbia, Department of Chemistry

Toward Point-of-Care Diagnostics with Consumer Electronic Devices: The Expanding Role of Nanoparticles

Eleonora Petryayeva and W. Russ Algar*

Department of Chemistry, University of British Columbia, 2036 Main Mall, Vancouver, British Columbia, V6T 1Z1, Canada.

*Corresponding author: algar@chem.ubc.ca

Abstract

There is a critical need for point-of-care (POC) diagnostics in health care and a parallel need for similar point-of-need (PON) diagnostics in other sectors. Such technology could have a profoundly positive impact on health, wellness and quality-of-life in both the developed and developing worlds. This very active area of research is converging with another very active area of research—the biomedical applications of nanotechnology—with exciting outcomes. In this review, we describe how nanoparticles facilitate the use of mass-produced consumer electronic devices for POC/PON diagnostic applications. We first highlight the growing need for POC diagnostics; provide a brief overview of clinical tests, biomarkers and lateral flow assays; describe the amenability of consumer electronic devices to POC/PON diagnostics; and summarize the attractive properties of nanoparticle materials in these contexts. Devices of interest include cell phones, smartphones, wearable technology, other CMOS imaging devices, scanners, optical drives/disc players, and strip readers. We continue to describe how nanoparticles can enable and enhance the readout of diagnostic assays with these consumer electronic devices using illustrative examples from the literature. The most utilized nanoparticles include gold nanoparticles, carbon nanoparticles, quantum dots, upconversion nanoparticles, polymer or silica nanoparticle composites with other materials, and viral nanoparticles. Given that assays combining the foregoing nanoparticles with consumer electronic devices have almost exclusively utilized optical readout, we further assess the potential for developing nanoparticle-

32   based electrochemical assays with readout through either a smartphone or personal blood glucose

33   meter (for non-glucose biomarkers). The review concludes with our perspective on future

34   research and development in this area, including the role nanoparticles may play in facilitating

35   the emergence of the smartphone as a leading personal health care device.

36

37   **List of Abbreviations**

38    $25(OH)D_3$ 25-hydroxyvitamin D
39   AChE   Acetylcholinesterase
40   A555   Alexa Fluor 555
41   ASV   Anodic stripping voltammetry
42   ATB_1 Aflatoxin B_1
43   Au NP   Gold nanoparticle
44   BRCA1/2   Breast cancer susceptibility gene 1/2
45   BRD   Blu-Ray disc
46   BSA   Bovine serum albumin
47   CAA   Circulating anodic antigen
48   CCD   Charge-coupled device
49   CD   Compact disc
50   CFU   Colony-forming unit
51   CIS   Contact image sensor
52   CMOS   Complementary metal-oxide-semiconductor
53   CRP   C-reactive protein
54   DNA   Deoxyribonucleic acid
55   dpi   Dots per inch
56   DPSS   Diode-pumped solid-state
57   DVD   Digital video disc
58   ELISA   Enzyme-linked immunosorbent assay
59   FDA   U.S. Food and Drug Administration
60   FRET   Fluorescence resonance energy transfer
61   GDP   Gross domestic product
62   hCG   Human chorionic gonadotropin
63   HIV   Human immunodeficiency virus
64   HRP   Horseradish peroxidase
65   ISO   International Standards Organization
66   LAMP   Loop-mediated amplification
67   LED   Light emitting diode
68   LFA   Lateral flow assay
69   LFIA   Lateral flow immunochromatographic assay
70   LFS   Lateral flow strip
71   LOD   Limit of detection
72   LTE   Long-term evolution wireless network
73   NASBA   Nucleic acid sequence-based amplification
74   NESA   Nicking endonuclease signal amplification

| 75 | NIDA | National Institute of Drug Abuse |
76	NIR	Near-infrared
77	NP	Nanoparticle
78	ODR	Optical darkness ratio
79	PCR	Polymerase chain reaction
80	Pdot	Polymer dots
81	*Pf*HRP2	*Plasmodium falciparum* histidine-rich protein 2
82	PIF	Parity inner failures
83	PL	Photoluminescence
84	PMT	Photomultiplier tube
85	POC	Point-of-care
86	PON	Point-of-need
87	PSA	Prostate specific antigen
88	QD	Quantum dot
89	RCA	Rolling circle amplification
90	RCSB	Research Collaboratory for Structural Bioinformatics
91	RGB	Red-green-blue
92	RNA	Ribonucleic acid
93	SMART	Signal mediated amplification of RNA technology
94	SPR	Surface plasmon resonance
95	TCP	3,5,6-trichloropyridinol
96	TMB	3,3′,5,5′-tetramethylbenzidine
97	TMPFP	Tetra-meso-fluorophenylporphine
98	UCNP	Upconversion nanoparticle
99	USB	Universal serial bus
100	UV(A)	Ultraviolet (A)
101	VNP	Viral nanoparticle

102

1. Introduction

104

105 Over the past decade, a rapidly growing trend has been the design of portable, low-cost bioassays

106 that use consumer electronic devices such as smartphones, digital cameras, scanners, and

107 CD/DVD/Blu-Ray disc players for quantitative readout of results. This trend is a new twist on an

108 older concept embodied by many strip reader devices, which, although not a consumer product

109 *per se*, can provide low-cost and portable readout of assays. The overarching objective of this

110 research is to enable a full range of point-of-care (POC) diagnostic tests that can improve the

111 efficiency and accessibility of health care globally, and eventually help realize personalized

112 medicine.[1, 2] The technical strategies used to address POC applications are often transferable

113 between health care and other sectors that stand to benefit from rapid on-site or field testing; for

114 example, environment, agriculture/aquaculture, food and water quality assurance, and public

115 safety and security, where such tests tend to be referred to as "point-of-need" (PON). Another

116 important trend over the past decade has been the application of nanotechnology to problems of

117 biomedical and analytical importance, where the unique properties of nanoparticles can increase

118 efficacy of therapies, improve analytical figures of merit in assays, and provide new

119 opportunities for research and development.[3-13] Not surprisingly, the above trends are converging

120 with exciting outcomes.

121

122 The general development and applications of POC/PON devices have been widely reviewed,[14, 15]

123 including assays for specific classes of analyte (*e.g.*, microbes,[16] cancer biomarkers,[17] toxins[18]),

124 specific analysis formats (*e.g.*, paper-based assays and devices,[19-23] lateral flow assays,[24] lab-on-

125 a-chip[25-27] and centrifugal microfluidic devices[25-27]), specific readout devices (*e.g.*, scanners,[28]

126 CD/DVD[29] and Blu-Ray[30] drives, smartphones[1, 31-33]), and specialized areas of development

127 (*e.g.*, paper-based assays with nanoparticles,[1, 31-33] immunoassays with nanoparticles,[34] and

128 microfluidic assays with gold nanoparticles[35]). In this review, we broadly discuss the

129 convergence of consumer electronic devices with nanoparticle materials for the development of

130 assays and diagnostics that are amenable to POC/PON settings. Figure 1 is a graphical overview

131 of the main content. The devices of interest include the aforementioned smartphones, digital

132 cameras, scanners, CD/DVD and Blu-Ray disc players, as well as strip readers and, to a limited

133 extent, blood glucose meters. Nanoparticles of interest include gold nanoparticles, quantum dots,

134 upconversion nanoparticles, silica and polymer nanoparticle composites, viral nanoparticles, and

135 carbon nanoparticles—all of which lend themselves to optical readout. To address important

136 concepts that recur throughout our review of the state of the art, we first summarize the need for

137 POC/PON diagnostics, provide a cursory overview of clinical diagnostic targets and lateral flow

138 assays, and describe the prospective utility of consumer electronic devices and the opportune

139 properties of the foregoing nanoparticle materials. We then outline the operating principles of

140 each consumer electronic device, including new developments in their analytical application, and

141 review examples of assays and diagnostics that combine nanoparticles with those devices,

142 highlighting important connections between device or assay capabilities and nanoparticle

143 properties. The extensive library of nanoparticles that are currently available offers remarkable

144 choice in selecting materials that can maximize the analytical performance of assays with

145   consumer electronic devices, providing exciting opportunities for current and long-term societal

146   impact in the context of POC/PON assays and diagnostics.

147
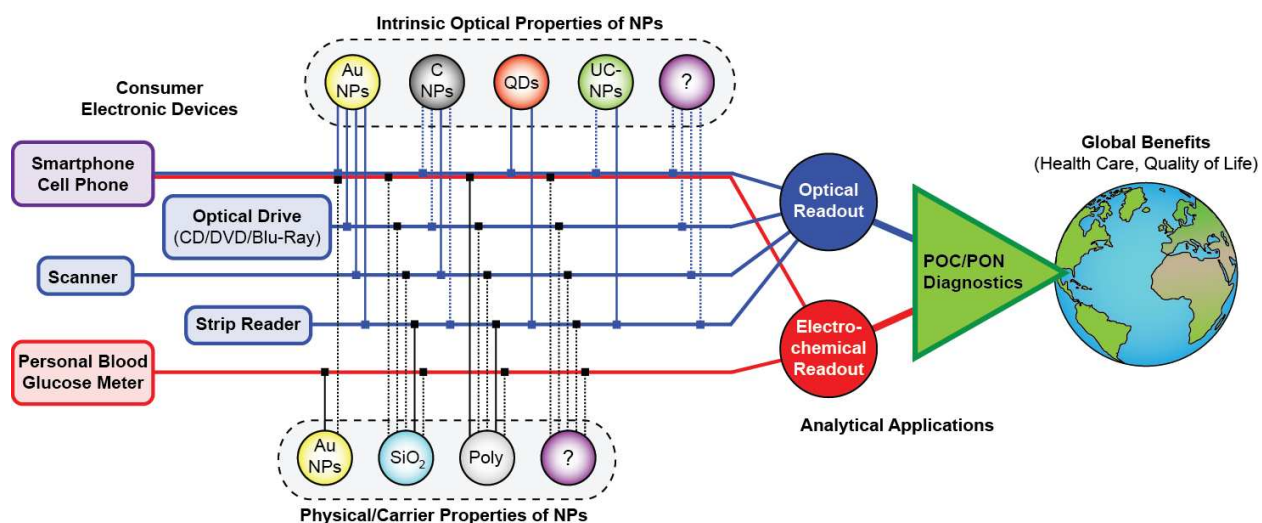
148

149   **Figure 1.** Graphical representation of the main content of this review, illustrating the convergence of
150   consumer electronic devices and nanoparticles for POC/PON diagnostics.
151

152   ## 2. Concepts

153

154   ### 2.1 The Need for Point-of-Care Diagnostics

155   The aim of POC diagnostic technology is to provide robust, portable, reliable, rapid, inexpensive

156   and simple testing of clinical biomarkers and other analytes. Minimization of the size, cost and

157   operational complexity of the analysis method and instrumentation is integral to this goal, but

158   achieving the best possible analytical figures of merit is not. Rather, it is sufficient to achieve

159   figures of merit that satisfy clinically relevant thresholds and ranges of analyte. It should also be

160   possible to easily transport and store consumables and devices (if any) at points of care without

161   loss of function. Both the U.S. Food and Drug Administration and the World Health

162   Organization have recommended criteria for POC diagnostics.[36-38]

163

164   POC diagnostic tests are needed in both developed and developing countries, where the current

165   models of health care delivery are unsustainable, albeit for different reasons. In developed

166   countries, advanced diagnostic technologies and services are readily available through

167   centralized laboratories that can be accessed by the public, typically at the direction of physicians

168   or during hospital stays. The demands on these services and their cost are such that the health

5

169   care expenditures in developed countries are a growing fiscal burden, amounting to 7–9% of the

170   gross domestic product (GDP) for G7 nations in 2012, with a projected increase to an average of

171   11% for advanced economies by 2050.[39, 40] Moreover, rural areas and remote areas of developed

172   countries tend to be underserviced compared to urban centres. Travel to urban centres for

173   medical testing creates extra stress for patients and adds further costs; for example, in 2010-

174   2011, the northern territory of Nunavut, Canada (pop. 33 000), had more than \$72M in health

175   care costs that were associated with travel and out-of-territory services.[41] An array of POC

176   diagnostic technologies that are sufficiently simple, rapid, reliable and economical to be

177   deployed in a physician's office or in patient's homes would be a tremendous step toward

178   increasing the efficiency of health care in developed countries.

179

180   In developing countries, the problem of accessibility to health care is greatly exacerbated, where

181   large populations may have little or no access to even the basic health services of the developed

182   world due to financial limitations, a shortage of skilled personnel, and a lack of infrastructure.[36]

183   The lack of infrastructure is not only with respect to biomedical and clinical equipment, but may

184   also include running water, refrigeration and electricity. In addition to basic medical tests and

185   screening for chronic disease, affordable test kits for infectious diseases can be a life-saving

186   intervention in many developing countries, where millions die every year due to inadequate

187   diagnosis and these tests could help prevent epidemics from turning into pandemics.[36]

188   Considering PON testing, rapid and low-cost methods of analysis for food safety and water

189   quality, counterfeit medicine, and veterinary testing are also needed.[20] Foodborne illnesses are a

190   direct result of ingestion of food contaminated with pathogens such as *Salmonella, E. coli*

191   *O157:H7*, and cholera, the latter of which affects 3–5 million people and kills more than 100 000

192   each year.[42] Non-existent protocols for water testing in rural areas also remains a major health

193   issue associated with diarrheal diseases.[43, 44] Contamination of drinking water supplies with

194   heavy metals (from industrial and mining production; *e.g.* mercury from gold mining),

195   agricultural pesticides and fertilizers, sewage, and other wastewater contaminants poses both

196   short-term and long-term health hazards. An estimated 50% of hospital patients worldwide suffer

197   from illness associated with contaminated water.[45] PON diagnostic tests for food and water

198   quality, and for early detection and screening of infectious disease, can improve life expectancy,

199   shorten recovery times and reduce treatment costs.[36, 46]

200

201   **2.2 Clinical Tests and Biomarkers**

202   To develop a comprehensive array of POC tests, it is necessary to detect a wide range of

203   biomarkers and analytes with often disparate technical requirements. Ideally, these tests would

204   use a common technology for quantitative readout, and would be able to directly analyze blood,

205   urine, sputum, saliva, and sweat samples—all with little or no user intervention and

206   straightforward readout of results. Most current clinical diagnostics do not meet these criteria.

207

208   Common classes of analytes in clinical diagnostics include blood gases (*e.g.*, O_2, CO_2), pH,

209   electrolytes (*e.g.*, Ca^{2+}, Mg^{2+}, Na^+, K^+, Cl^-), transport proteins (*e.g.*, lipoproteins, ceruloplasmin,

210   transferrin, haptoglobin, haemoglobin), metabolites (*e.g.*, glucose, creatinine, urea, lactate),

211   enzymes   (*e.g.*,   creatine   phosphokinase,   alkaline   phosphatase,   aspartate/alanine

212   aminotransferase), vitamins (*e.g.*, beta-carotene; vitamins A, B12, C and 25-hydroxyvitamin D),

213   hormones (*e.g.*, thyroid stimulating, follicle stimulating, testosterone, estrogen), cytokines (*e.g.*,

214   interleukins; tumour necrosis factor), therapeutic drugs (*e.g.*, digoxin, perhexiline, cyclosporine,

215   tacrolimus), drugs of abuse (*e.g.*, amphetamines, barbiturates, benzodiazepines, cannabinoids,

216   opiates), cardiac and inflammatory markers (*e.g.*, C-reactive protein, troponin I, myoglobin),

217   genes (*e.g.*, BRCA1 and BRCA2 breast cancer genes), and infectious agents and pathogens (*e.g.*,

218   influenza, measles). Conventional laboratory procedures for assaying these analytes are often

219   complex. Sample processing can be labourious and require specialized training, and the analyses

220   often utilize instrumentation that is expensive, non-portable, and operated by skilled technicians;

221   for   example,   spectrophotometric,   electrochemical   and   chromatographic   measurements,

222   molecular biology techniques, cell culture and counting, among many other methods.[47] Notable

223   exceptions to the above are lateral flow assays, which are much more amenable to POC

224   applications, as described in Section 2.3.

225

226   The above classes of analyte can be reduced to three basic groups that can address most

227   diagnostic needs: proteins, nucleic acids, and small molecules.

228

229   Proteins, whether enzymes, antibodies, certain hormones, cytokines, or otherwise, are frequent

230   targets of POC diagnostics. The RCSB protein databank lists > 100 000 entries from various

231   species,[48] and more than 18 000 or 92% of gene-encoded human proteins have been catalogued,

232   as well as many proteins from pseudogenes and non-coding RNA.[49-52] Depending on the target,

233   protein biomarker concentrations typically range from picomolar to micromolar in bodily fluids.

234   In the case of enzymes, their activity may also be of interest in addition to their concentration, in

235   which case a product of that enzymatic activity is measured. When concentration is of interest,

236   the biorecognition elements that are the basis for protein-targeting assays are usually antibodies,

237   aptamers, or ligands that selectively bind to the target protein. Certainly, the standard format for

238   protein detection is an immunoassay such as an enzyme-linked immunosorbent assay (ELISA),

239   which has been one of the most prominent clinical laboratory tests over the past 20 years. As

240   biorecognition elements, antibodies have remained indispensible because of their specificity and

241   affinity but have several potential drawbacks, including limited stability, batch-to-batch

242   variability, and high production costs. In many ways, aptamers are preferable biorecognition

243   elements for POC/PON assays because they are more robust and more economically produced;[53,]

244   [54] however, aptamers that have affinity comparable to antibodies are not yet known for many

245   target proteins.

246

247   Nucleic acid assays are increasingly important for the diagnosis of disease, identification of

248   pathogens, and identification of genetic conditions and predispositions. Genes can be useful

249   biomarkers for organisms and their physiology, and are sometimes preferable biomarkers over

250   the proteins that they encode. Many thousands of genomes from eukaryotes, prokaryotes and

251   viruses have been completely or partially sequenced,[55] including the estimated 19 000 protein-

252   coding human genes.[56] The analysis of DNA and RNA directly from bodily fluids is limited by

253   its very small amount (*e.g.*, 10^2–10^{11} copies per 1 mL of blood), necessitating multiple

254   preparatory steps prior to analysis (*e.g.*, extraction, purification and amplification).

255   Conventionally, polymerase chain reaction (PCR) is used for amplification of DNA. The

256   thermocycling inherent to this process is not ideal for POC/PON applications, although

257   computer-based thermocycling is possible.[57] Alternatively, there are now amplification

258   techniques that do not require thermocycling and may thus be more compatible with POC/PON

259   applications. As reviewed recently,[58] these isothermal techniques include loop-mediated

260   amplification (LAMP), rolling circle amplification (RCA), nucleic acid sequence-based

261   amplification (NASBA), signal mediated amplification of RNA technology (SMART), nicking

262   endonuclease signal amplification (NESA), and several others. Synthetic oligonucleotides that

263   are complementary to the sequence of target genes are typically used as biorecognition elements,

264   and are robust and relatively inexpensive.

265

266   The most common small molecule targets for diagnostics are metabolites such as hormones,

267   vitamins, amino acids, sugars, and other small organic molecules. The Human Metabolome

268   Database lists *ca.* 42 000 entries,[59, 60] and many of these can serve as indicators of disease.

269   Similar to proteins, some metabolites are found at high concentrations (>1 mM), at low

270   concentrations (<1 nM), and concentrations in between. The most common biorecognition

271   element for metabolites are antibodies, although the small size and similar chemical structures of

272   these analytes often yield limited sensitivity and specificity, including cross-reactivity, that

273   makes immunoassay-based detection challenging. Aptamers are again promising alternatives to

274   antibodies in these assays, but are still limited by the number of aptamers available and their

275   affinity for their small molecule targets.

276

277   Another diagnostic test of interest is the detection of specific cell types and microorganisms; for

278   example, pathogens that cause disease. Six common types of pathogens include viruses, bacteria,

279   fungi, prions, protozoans and parasites. Infectious diseases contribute to more than 95% of all

280   death in developing countries, and include human immunodeficiency virus (HIV), malaria

281   (*Plasmodium* parasite), tuberculosis (*Mycobacterium tuberculosis*), and hepatitis A/B virus.[61]

282   Moreover, at the time of writing, the worst recorded *Ebola* virus outbreak in history has infected

283   >8 000 people and killed more than 5 000 people, mostly in West Africa.[62] Although pathogen

284   outbreaks in the developed world are relatively rare and generally minor, there are nonetheless

285   recurring instances of contamination of food with *Salmonella*, *Staphylococcus aureus*, *Listeria*

286   *monocytogenes* and *E.coli O157:H7* pathogens.[63, 64] The gold standard methods for detecting

287   pathogens are culture-based assays that provide good sensitivity and selectivity, but require long

288   incubation times that limit rapid responses to outbreaks.[65] An alternative strategy for more rapid

289   analysis is to target protein, nucleic acid, and small molecule biomarkers that are pathogen

290   specific.

291

292   The above discussion on health-related targets for diagnostics is by no means comprehensive,

293   and there is also significant demand for molecular diagnostic tests beyond health care. For

294   example, public service employees are often tested for illegal recreational drugs, and elite

295   athletes are tested for performance-enhancing substances. Many heavy metals and small

296   molecules such as pesticides and other toxic pollutants are important targets in environmental

297   analysis,[66] while rapid monitoring and diagnostic tests are also valuable tools for biofuel

298   production and other non-health areas of the biotechnology sector.[67, 68] Many of the approaches

299   and challenges described for health-related diagnostics are equally applicable to these other

300   sectors, and *vice versa*.

301

302   **2.3 Lateral Flow Assays**

303   Lateral flow assays have been one of the most successful and POC-amenable formats since the

304   introduction of lateral flow immunochromatographic assays in 1988 by Unipath.[69] This format

305   combines concepts from paper chromatography and immunosorbent assays. It frequently does

306   not require the additional washing steps of the latter and typically needs only ~0.1 mL of sample.

307   LFA devices are suitable for the direct analysis of blood samples as plasma components are

308   separated from blood cells within minutes, and are also suitable for the analysis of urine and

309   other bodily fluids. Routinely used, commercially available POC immunochromatographic tests

310   include those for pregnancy (human chorionic gonadotropin level) and ovulation; infectious

311   diseases (*e.g.*, malaria, influenza, HIV); drugs of abuse (*e.g.*, NIDA-5 panel for cannabinoids,

312   cocaine, amphetamines, opiates and phencyclidine); and cardiac biomarkers (*e.g.*, troponin I,

313   creatine kinase-MB, myoglobin).

314

315   Lateral flow immunochromatographic assay strips consist of a sample application pad, a

316   conjugate pad, a membrane (*e.g.*, nitrocellulose, cellulose), and an absorbent pad, as shown in

317   Figure 2.[18, 20, 70] Reporter antibodies conjugated with a contrast-providing reagent (dye-stained

318   latex beads originally[71]) are deposited but not immobilized on the conjugate pad. A fluid sample

319   is applied to the sample pad and wicks down the length of the test strip. As the sample passes

320   through the conjugate pad, the contrast reagent-reporter antibody conjugates bind to the target

321   analyte. Further along the strip, the target analyte also binds to capture antibodies immobilized in

322   the test zone, resulting in retention of the contrast label. Colour imparted to the test zone by the

323   contrast label indicates the presence of target analyte in the sample. A control zone also tends to

324   be included on the membrane, and this zone contains antibodies that bind to the reporter

325   antibody. The absorbent pad ensures steady wicking of the sample fluid along the test strip.

326   Many variations of this general assay design are possible; common variations include

327   substitution of antibodies with other biorecognition elements, or the use of a competitive assay

328   format rather than a sandwich assay format.

329
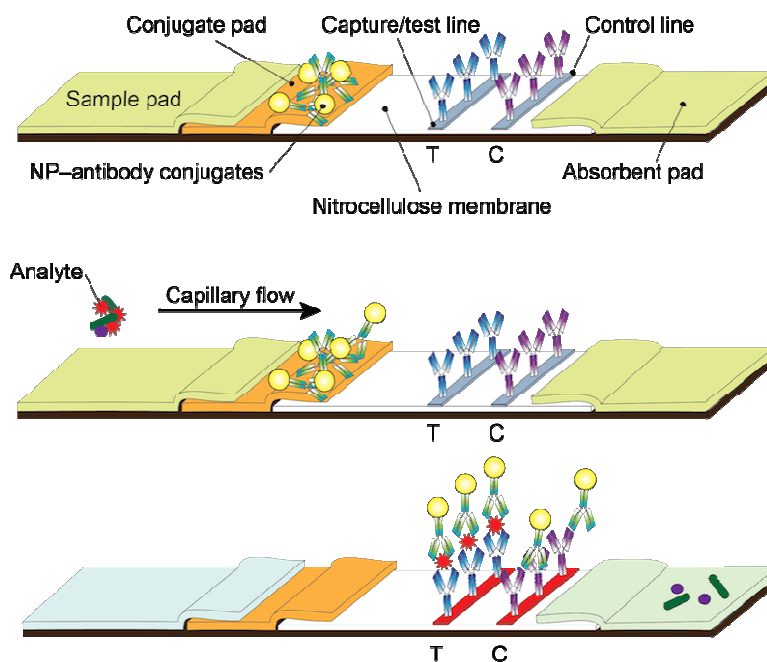
330

331   **Figure 2**. Basic design of a lateral flow immunochromatographic assay (LFIA). The device comprises a
332   sample pad, conjugate pad, detection zone with test (T) and control (C) lines, and an absorbent pad. The
333   sample containing analyte is added to the sample pad and drawn towards absorbent pad by capillary
334   action. NP-antibody conjugates bind to analyte (antigen) present in the sample and are captured on the
335   test line, whereas NP-antibody conjugates that have not bound antigen are captured on the control line.

336

337   Although dye-stained latex beads are still used to generate contrast in lateral flow assays, many

338   commercial assays now use gold nanoparticles, and additional nanoparticle materials have been

339   investigated as contrast reagents in research toward new or improved diagnostics. There is also

340   an increasing demand for quantitative rather than qualitative results from lateral flow assays, and

341   this quantitation is often possible through analysis of digital images instead of simple visual

342   inspection. Lateral flow assays feature prominently in Section 3, where recent research is

343   reviewed. For brevity in that section, we define three abbreviations related to this assay concept:

344   the general method, a lateral flow assay (LFA); the most common variant, a lateral flow

345   immunochromatographic assay (LFIA); and the device itself, a lateral flow strip (LFS).

346

347   **2.4 Utility of Consumer Electronic Devices**

348   Whether in the developed world or the developing world, modern consumer electronic devices

349   can help address challenges in POC/PON testing in three principal ways: (i) lower equipment

350   and infrastructure costs; (ii) miniaturization and portability; and (iii) data processing, storage and

351   communication. The most common devices, which include scanners, CD/DVD and Blu-Ray

352   players, web cams, cell phones and smartphones, offer the foregoing benefits to different degrees

353   and have different suitability for the developed world *versus* the developing world.

354

355   In the developed world, all of the above devices share the benefit of low cost, which arises from

356   their mass production and a highly competitive marketplace. Prices typically range from $10–

357    $1000 depending on the device and much of the developed world already owns one or more of

358   these devices. In the United States, for example, ownership statistics are 80% for DVD/Blu-Ray

359   players, 64% for laptop computers, 57% for desktop computers, 45% for cell phones, and 62%

360   for a smartphone (2013 data).[72] In the developing world, one wishes to discuss cost in terms of

361   cents rather than dollars; however, it must be recognized that the main role of consumer

362   electronic devices in a POC/PON test will be quantitative readout and data handling, and these

363   devices remain among the best candidates for establishing a frontline of health care

364   infrastructure, particularly if the corresponding consumables for diagnostic tests cost pennies and

365   also support qualitative assessment when these devices are not available. Moreover, these

366   devices are not beyond the reach of the developing world as some people in these countries have

367   easier access to mobile phone technology than they do to clean water.[73]

368

369   From a technical perspective, scanners offer large-area colour imaging with reproducible

370   positioning and illumination. Many current models of scanners are compact, support wireless

371   communication, and can be fully operated *via* a USB connection to a laptop or notebook

372   computer. Disc players are common household items and optical drives are widely available as

373   built-in or peripheral components of laptop/notebook computers. Discs also offer a substrate for

374   arraying assay zones (*e.g.*, microarray format) and integrating microfluidic channels, while disc

375　players and drives offer optical readout and spinning motion that provides a centripetal force
376　suitable for driving fluid flow. Cell phones, and later smartphones (the distinction being that
377　smartphones have an operating system), have undergone remarkable technological growth over
378　the last two decades. The first cell phone, the Motorola DynaTAC, became commercially
379　available in 1984. It weighed 790 g and was 25 cm in length with a price of $4 000 (*ca.* $10 000
380　in 2014 dollars).[74] The current generation of smartphones, such as the best-selling Samsung
381　Galaxy and Apple iPhone models, offer immensely greater capabilities at a fraction of the price
382　and a fraction of the size ($600–$1000, 130 g). These capabilities include high-quality built-in
383　cameras, multiple modes of wireless communication (*e.g.*, WiFi®, Bluetooth, LTE), global
384　positioning systems, security features, excellent data storage capacity, processing and graphics
385　power to support software applications (apps), and many hours of battery life.
386

387　In the context of POC/PON diagnostics, smartphones are leading candidates to fulfil the role of
388　computers in modern laboratory instrumentation, with lower cost and greater portability than
389　notebook/laptop computers (which have built-in webcams and similar wireless connectivity).
390　Furthermore, although a POC/PON test may be simple enough for a minimally skilled technician
391　or unskilled person to conduct, determining a diagnosis or prognosis from test results may not
392　always be as straightforward. Smartphone apps can potentially automate sample logging and data
393　processing, and store or send results for subsequent interpretation by medical professionals or
394　other highly-skilled personnel, whether locally or across the world. Importantly, these devices
395　are also globally ubiquitous with 1.5 billion mobile telecommunications subscribers in the
396　developed world and 5.4 billion in the developing world,[75] albeit that the latter are primarily cell
397　phone users rather than smartphone users.
398

399　**2.5　Optical Properties of Nanoparticles**
400　While consumer electronics can provide a means of assay readout, these devices cannot generate
401　the readout signal or contrast themselves. These signals must come from selective recognition
402　chemistry that is directly or indirectly coupled to a physical process that generates a measurable
403　output. Nanoparticles (NPs) can be used for the generation of these signals and provide
404　enhancements or advantages over molecular reagents. By definition, NPs are particles that are
405　less than 100 nm in their largest dimension,[76] although here we stretch the definition to include

406   particles with dimensions of hundreds of nanometers. The small size and molecule-like diffusion

407   of NPs is complemented by large surface area-to-volume ratios, interfaces that can be further

408   functionalized, and, in the case of many NP materials, size-dependent properties that are either

409   not observed with their bulk analogues or are significantly enhanced. Table 1 briefly summarizes

410   the key features of some NP materials that are currently used in POC/PON diagnostics or which

411   are promising candidates for future use. Given the nature of the consumer electronic devices

412   described above—in particular their optoelectronic features—we limit the present discussion to

413   optically active NP materials and briefly discuss other NP materials in Section 4.

414

415   <<Refer to end of document for Table 1>>

416

417   From the standpoint of optical diagnostics, there are many NP materials of interest. At present,

418   the three most common materials are gold NPs (Au NPs), quantum dots (QDs), and lanthanide-

419   based upconversion nanoparticles (UCNPs).

420

421   Au NPs have plasmon bands in their UV-visible absorption spectrum and exhibit strong light

422   scattering that increases with increasing NP size (Figure 3A).[3, 5, 77] These properties manifest as

423   an intense red colour for assay readout with sensitivity that typically exceeds that of dyes and

424   other materials. Although this red colouration can be seen by the naked eye and provide

425   sufficient sensitivity for many assays, limits of detection (LOD) can be improved by orders of

426   magnitude with signal amplification strategies such as silver enhancement, which increase the

427   optical contrast of the test zone. The silver enhancement strategy was popularized by Mirkin and

428   coworkers[78] and relies on the reductive deposition of silver on Au NPs, thereby increasing the

429   nanoparticle size and extinction coefficient, darkening their macroscopic appearance on a white

430   background. The first and compelling demonstration of this strategy was the detection of 50 fM

431   of target DNA with scanner readout.[78] Silver enhancement remains commonplace for POC

432   diagnostic assays with scanners, as well as other consumer electronic devices. Alternatively,

433   amorphous carbon NPs appear black and, like silver-enhanced Au NPs, provide high contrast

434   under white-light illumination.[79]

435

436   QDs exhibit bright, size-dependent photoluminescence (PL) that is easily excited and can be
437   tuned across a wide spectral range (Figure 3B).[6-8] The optical properties of QDs are generally
438   considered to be superior to those of fluorescent dyes: their light absorption is much stronger and
439   more spectrally broad, and their emission is much more spectrally narrow and resistant to
440   photobleaching. Lanthanide-based upconversion nanoparticles (UCNPs) convert near-infrared
441   (NIR) excitation into visible emission, the colour of which depends on their composition (Figure
442   3C).[10-12] Upconversion is not possible with fluorescent dyes. With both QDs and UCNPs, their
443   light emission against a dark background provides contrast for assay readout. Further properties
444   of QDs and UCNPs that make them advantageous for POC/PON assays with consumer
445   electronics, and in comparison to fluorescent dyes and other materials, are described in the
446   context of specific examples in Section 3. More generally, the benefits of fluorescence detection
447   in POC/PON assays include potentially greater sensitivity and lower LODs, potentially greater
448   tolerance of sample colouration, and new possibilities for multiplexed analyses. The trade-off is
449   that fluorescence measurements are somewhat more technically demanding, requiring an
450   excitation light source and readout against a dark background (*i.e.*, exclusion of ambient light).
451   Fortunately, POC/PON-amenable light sources are widely available (see Section 3.1) and 3D
452   printing provides a convenient means of producing light-blocking enclosures or attachments for
453   smartphones or other complementary-metal-oxide-semiconductor (CMOS) image sensor devices.
454
455   Other NP materials that are of interest in context of POC/PON diagnostics are silica NPs[80-82] and
456   polymer NPs.[83, 84] However, in contrast to the preceding materials, it is their physical properties
457   that are of interest rather than their optical properties. These NPs, which can have dimensions of
458   hundreds of nanometers, can serve as carriers of molecules or smaller NPs that provide contrast
459   (*e.g.*, Au NPs, QDs, UCNPs). Viral NPs and genome-free virus-like NPs (collectively, VNPs)
460   can also serve as carriers of contrast reagents, with the benefit of being monodisperse, tailorable
461   through genetic engineering and chemical functionalization, and producible at a large scale.[85, 86]
462   Analogous to the original use of latex beads as a carrier for dye molecules, the concept is that
463   many NP contrast reagents can be associated with a single binding event even though there will
464   be no more than one carrier particle per binding event, resulting in greater sensitivity.
465

A Au NPs

B QDs

C UCNPs
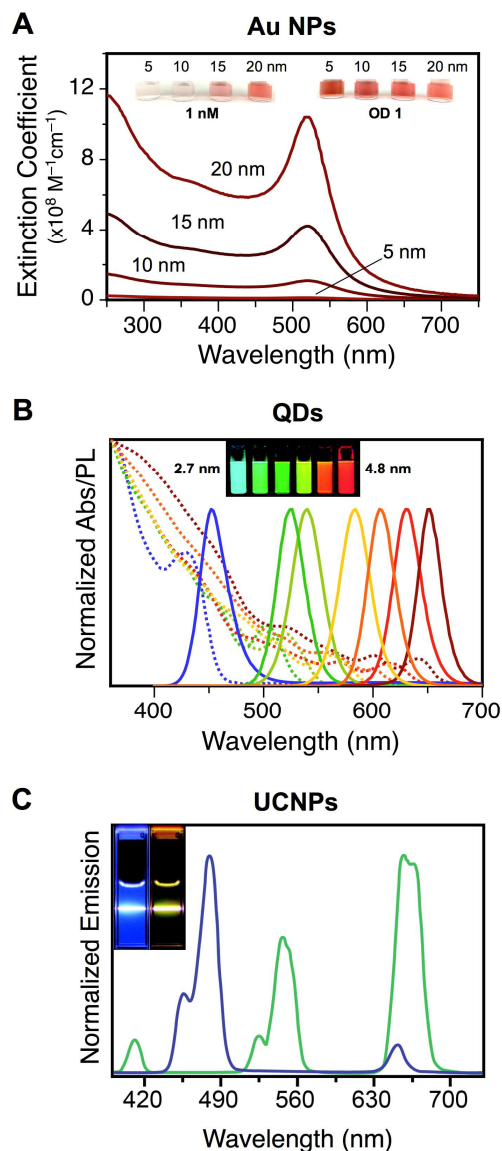
Figure 3. (**A**) Size-dependent molar extinction coefficient of Au NPs as a function of wavelength. The inset photographs show solutions of 5, 10, 15 and 20 nm Au NPs at 1 nM concentration and with an optical density of 1 (*ca.* 90, 10, 3, and 1 nM concentrations for 5, 10, 15 and 20 nm Au NPs, respectively). (**B**) Size/composition-tunable absorbance and emission of CdSe/ZnS and CdSeS/ZnS QDs. The inset photograph shows samples of different sizes of CdSe/ZnS QDs under UVA (365 nm) illumination. Photograph reprinted with permission from ref.[87] Copyright 2011 American Chemical Society. (**C**) Upconversion emission spectra of $NaYF_4$:Yb/Tm (20/0.2 mol %; blue line) and $NaYF_4$:Yb/Er (18/2 mol %; green line) nanoparticles. The inset photographs show samples of these nanoparticles under 980 nm excitation with a diode laser (600 mW). Adopted with permission from ref.[88] Copyright 2008 American Chemical Society.

479   Several other optically-active NP materials are known and, to our knowledge, have yet to be

480   utilized for POC/PON assays with consumer electronic devices. For example, carbon

481   nanotubes,[89, 90] graphene oxide,[91, 92] carbon dots,[93, 94] and nanodiamonds[95, 96] exhibit PL that can

482   be useful for biological imaging and assays; however, it is not clear that the characteristics of this

483   PL (*e.g.*, brightness, spectral range of absorption and emission) is well-suited to readout with

484   consumer electronic devices. On the other hand, semiconducting polymer nanoparticles (Pdots)[97]

485   have exceptionally bright PL that is certainly promising for readout with consumer electronic

486   devices, and the lack of examples to date is likely a product of the novelty of the materials.

487   Beyond optical properties, many NP materials also have magnetic or electrochemical properties

488   that are of interest. These materials are not considered in this review, with the exception of

489   briefly revisiting electroactive NP materials in Section 4. It should also be noted that NP

490   materials are utilized in POC/PON assays as bioconjugates. The preparation and characterization

491   of these bioconjugates, while not discussed here, is critically important to assay development and

492   non-trivial. Recent reviews have addressed methods available for both the bioconjugation of

493   NPs[98] and the characterization of those bioconjugates.[99]

494

495

496   ## 3. Bioassays with Consumer Electronics and NPs

497

498   This section describes consumer electronic components and devices that are being actively

499   developed as platforms for readout of POC/PON diagnostics and assays. Light-emitting

500   electronic components, which are common to all of the assays considered, are first reviewed,

501   then, for each consumer electronic device, the basic design elements and functional principles

502   underlying its utility as a readout platform are described, followed by examples of assays that use

503   that device in combination with NPs for readout of results. We have strived to provide many

504   representative examples; however, the text is not exhaustive and we apologize to researchers

505   whose valuable contributions we have unintentionally overlooked.

506

507   ### 3.1 Light Sources

508   As will be seen, common light sources for POC/PON assays with NPs include white or coloured

509   light-emitting diodes (LEDs), laser diodes and, to a lesser extent, hand-held ultraviolet (UV)

510   lamps or "black lights." These light sources permeate the developed world and are available low

511   price points. LEDs are ubiquitous as indicator lights and display backlights in electronic devices,

512   in traffic signals and signage, and in both decorative and ambient lighting products. Laser diodes

513   are critical components of optical drives/disc players, printers, barcode scanners, manufacturing

514   technology, telecommunication systems, and are also used in medicine and dentistry. Hand-held

515   UV lamps that emit long-wavelength UVA light have been traditionally used for forgery

516   detection (*e.g.*, monetary bills, documents) but are gradually being replaced by LEDs that emit in

517   the same spectral range. All of these light sources can be battery-operated for extended periods,

518   which is a critical consideration for use in POC/PON applications.

519

520   Of the above light sources, LEDs are the most economical ($0.01–$1.00 typical) and the most

521   amenable to miniaturization (millimetre dimensions). LEDs usually have low operating voltages

522   (3–5 V) and low power consumption ($\sim 10^{-3}$–10^{-2} W), although higher-power LEDs ($>10^{-1}$ W)

523   are available at greater cost than noted above. Low-cost, low-power LEDs are the most relevant

524   to POC/PON applications. The emission from an LED is incoherent and distributed over a

525   relatively wide angular range. Its peak emission wavelength, which may be in the UV, visible or

526   infrared region of the spectrum, is determined by the semiconductor composition of the diode.

527   Spectral full-widths-at-half-maxima (FWHM) are typically in the range of *ca.* 15–50 nm.

528   Representative examples of some low-cost LED spectra are shown in Figure 4A. Whereas colour

529   LEDs (particularly blue and UV wavelengths) are well-suited to readout of photoluminescence,

530   white-light LEDs are well-suited to colourimeric readout. Most white-light LEDs are actually

531   blue LEDs with a phosphor coating that has broadband emission in the green-red region of the

532   spectrum, as shown in Figure 4B. Colourimetric readout is also possible with a combination of

533   red, green and blue LEDs.

534

535   Diode lasers provide more intense illumination than LEDs and have coherent, monochromatic

536   emission (FHWM < 1 nm). From the perspective of POC/PON applications, laser diodes of the

537   type found in laser pointers ($\sim 10^{-3}$ W) and optical disc drives and players ($\sim 10^{-1}$ W) are the most

538   relevant. Figure 4C shows the emission from laser diodes that are commonly used for excitation

539   of photoluminescence, including violet (405 nm), blue (447 nm), green (532 nm), red (650 nm)

540   and infrared (980 nm) wavelengths. Note that many green laser diodes are actually infrared laser

541   diodes that have been frequency doubled and fitted with an IR-blocking filter (DPSS lasers).

542

543 Hand-held, battery-operated UVA lights are another light source that is potentially suitable for

544 POC/PON applications. These sources are low-pressure mercury discharge lamps where a

545 phosphor converts the 254 nm emission from mercury to 365 nm emission from the lamp. A

546 coating on the quartz tube absorbs any visible light. Power consumption is typically on the order

547 of a few watts. The principal benefit of these sources is that relatively large areas can be

548 illuminated with spectrally narrow light (FWHM ~15 nm, Figure 4D). Although "mini" or "pen"

549 lamps are commercially available, UVA lights are less amenable to miniaturization than LEDs or

550 diode lasers.

551
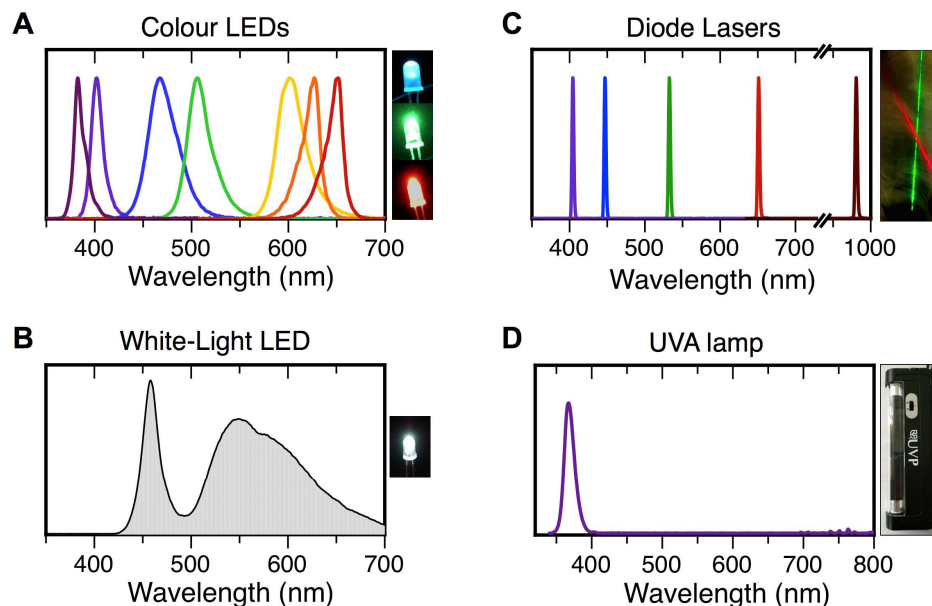
552

553 **Figure 4.** Emission spectra of commercial light sources well-suited to POC/PON diagnostics: **(A)** various
554 colour LEDs emitting in UV-visible region of the spectrum; **(B)** white-light LED; **(C)** five common
555 wavelengths of laser diodes (the FWHM > 1 nm is a measurement artefact); and **(D)** and a UVA lamp or
556 "black light."

557

558

559 **3.2 CMOS Image Sensors: Digital Cameras to Smartphones**

560

561 **3.2.1 Technology**

562 Modern CMOS image sensors are compact, provide high image quality, and are widely

563 incorporated into consumer devices such as cell phone and smartphone cameras; webcams;

564 wearable technology (*e.g.*, Google Glass, Sony's SmartEyeglass); and digital cameras for
565 traditional photography, hobbies (*e.g.*, Raspberry Pi), and recreational activities (*e.g.*, GoPro). A
566 selection of these devices are shown in Figure 5A. CMOS technology has also permeated
567 scientific research in the form of microscopy cameras. The primary advantages of CMOS sensors
568 over charge-coupled device (CCD) sensors are full integration of circuitry (which is more
569 amenable to miniaturization), lower power consumption, and faster frame rates. Originally, these
570 advantages were at the expense of image quality; however, improvements in fabrication
571 technology and consumer demands for increasing performance from their mobile devices have
572 driven the advancement of CMOS technology to its current pinnacle.

573
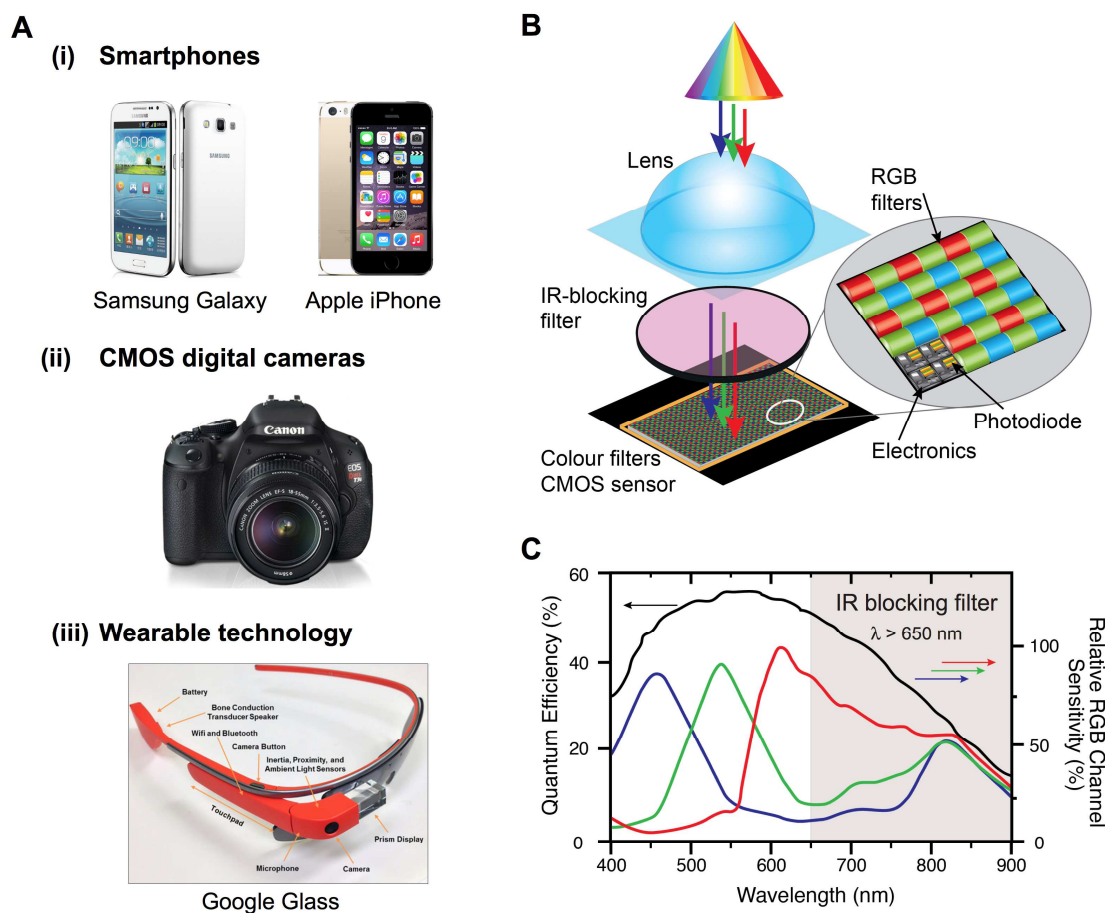
574
575 **Figure 5. (A)** Examples of consumer electronic devices equipped with CMOS cameras: (i) smartphones;
576 (ii) digital cameras; and (iii) wearable devices. The image in (iii) is reproduced with permission from ref.[100].
577 Copyright 2014 American Chemical Society. **(B)** Simplified schematic of a CMOS image sensor.
578 **(C)** Spectral sensitivity of a typical CMOS image sensor without (black) and with RGB colour filters
579 (coloured lines). The typical blocking region of an IR filter is also shown.

20

580

581   As shown in Figure 5B, a CMOS image sensor has two main optical components: a pixel sensor

582   array and optical filters for colour transmission (*e.g.*, Bayer filter) and blocking UV and IR light.

583   Millions of pixels capture light and convert that light into a voltage proportional to its intensity,

584   where each pixel has its own amplification and digitization circuitry. CMOS sensors have

585   wavelength-dependent sensitivity between *ca.* 380–1100 nm, as shown in Figure 5C. Colour

586   information is obtained by superimposing an array of bandpass filters that transmit either blue,

587   green or red light on the pixel array. The most common filter pattern is the "Bayer mosaic,"

588   which is a repetitive 2×2 grid with one red filter, two green filters, and one blue filter per four

589   pixels. This ratio of filters was designed to mimic the human eye's greater sensitivity to green

590   light.[101] IR and UV filters can be added to block unwanted wavelengths of light from outside the

591   visible spectrum. Electronics and demosaicing algorithms convert the pixel signals into digital

592   colour images.

593

594   **3.2.2 Growing Analytical Applications**

595   CMOS-based cameras, especially those in smartphones, have emerged as promising tools for

596   heath care and bioanalysis over the past few years. Numerous smartphone apps and accessories

597   have become available to assist the general public with basic health monitoring; for example,

598   heart rate,[102, 103] blood pressure,[102] body mass index,[102] and detection of ear infections[104] and

599   potential skin cancer.[105, 106] Initial evidence suggests that smartphone technology can support

600   better health outcomes, as demonstrated with apps that promote physical activity and weight

601   loss.[107, 108] Smartphone imaging has also been investigated as a POC/PON readout platform for

602   molecular diagnostics such as immunoassays,[109-111] nucleic acid hybridization assays,[112] and

603   colorimetric assays for cholesterol,[113] food allergens,[114] enzymes[115] and various urinary, salivary

604   and sweat biomarkers.[116, 117] Digital images acquired with a smartphone camera can be analysed

605   to extract quantitative information, most frequently in terms of the grayscale or RGB colour

606   intensities for pixels of interest. These analyses can be done with computer-based image analysis

607   software designed for either scientific research or consumer use (*e.g.*, Adobe Photoshop),

608   including freely available software (*e.g.*, ImageJ), as well as smartphone apps.

609

610 Analytical and biological applications of cell phone and smartphone cameras also go beyond
611 macroscopic digital photography. For example, when these cameras are combined with
612 additional optics, they can be used for dark-field and bright-field microscopy of cells.[118] Imaging
613 of a single fluorescent polystyrene NP (100 nm diameter) has also been demonstrated by the
614 Ozcan Laboratory using a smartphone (Nokia PureView 808).[119] The phone was equipped with a
615 high-resolution CMOS sensor (41 MP) and utilized oversampling technology (*i.e.*, pixel binning)
616 that enabled capture of five times more light than a typical zoom camera. A compact attachment
617 to the phone was fabricated using 3D printing technology; it integrated a 405 nm laser diode
618 excitation source (75 mW) powered by three 1.5V batteries (AAA size), a longpass filter to
619 remove scattered excitation light, a 2× magnification lens, and optomechanics for focus
620 adjustment (Figure 6A).

621
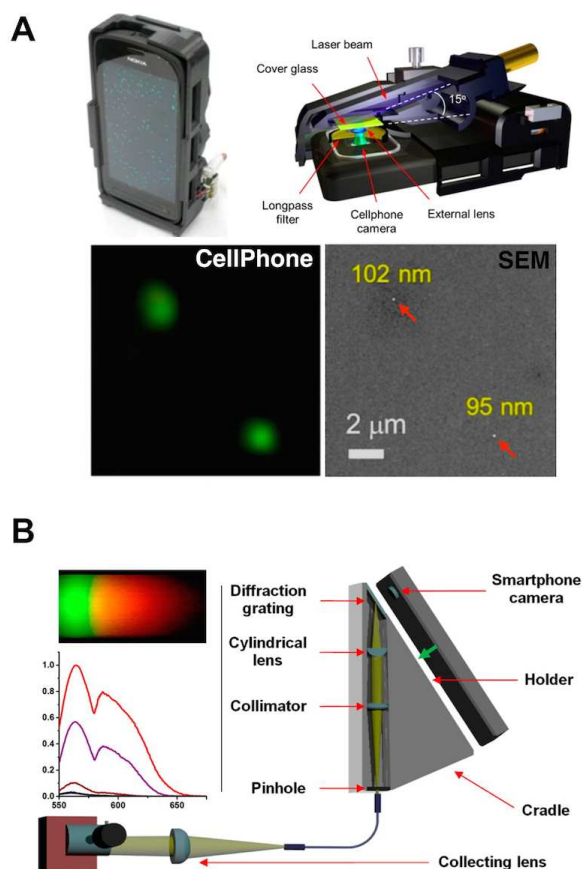
622
623 **Figure 6. (A)** Cell phone-based fluorescence imaging of individual NPs and viruses: (i) Front view of the
624 smartphone microscope and a schematic diagram of its components; (ii) Images of 100 nm fluorescent
625 NPs acquired with the cell phone show excellent agreement with SEM images. Adapted with permission
626 from ref.[119] Copyright 2013 American Chemical Society. **(B)** Attachment that enables use of a smartphone

627 as a spectrophotometer for fluorescence emission measurements. The key component is a transmission
628 diffraction grating. Reprinted with permission from ref.[120] Copyright 2014 American Chemical Society.

629

630

631 Smartphone cameras can also be used as spectrographs.[121] As an example, the Cunningham

632 Laboratory developed a simple transmission grating interface for a smartphone camera

633 (iPhone 4) that enabled acquisition of full fluorescence emission spectra (Figure 6B).[120] The

634 diffraction grating (1200 lines/mm) dispersed fluorescence excited with a green diode laser

635 pointer onto the camera. Due to built-in UV and IR blocking filters, the smartphone camera-

636 spectrophotometer was sensitive over the spectral range *ca.* 400–700 nm with a spectral

637 dispersion of ~0.3 nm/pixel. Tests with a molecular beacon assay for microRNA demonstrated a

638 LOD of 1.3 pM, which was superior to a 3.6 nM LOD obtained with a conventional

639 spectrofluorimeter. The observed enhancement was a combined effect of the greater quantum

640 efficiency of the CMOS sensor in the smartphone *versus* the photomultiplier tube (PMT) in the

641 spectrofluorimeter (40% *vs.* 12%, not accounting for PMT amplification), as well as a more than

642 30 000-fold increase in excitation efficiency. The latter was a result of the greater output power

643 of the diode laser source (~300 mW) *versus* the xenon lamp in the spectrofluorimeter (10 µW),

644 and a more than 300-fold smaller illumination volume with laser excitation. The Dana

645 Laboratory has demonstrated that a smartphone camera can also be integrated into a confocal

646 Raman system for detection of the surface enhanced Raman scattering spectrum from ethanol.[122]

647 Raman spectra were acquired with green laser excitation (532 nm, 10 mW) by placing a

648 collimator and transmission grating in front of the camera sensor, which had overall sensitivity

649 comparable to CCD and PMT detectors. Observation of blinking events from single molecules

650 diffusing in and out of hot spots on a silver nano-island plasmonic substrate were observed with

651 the smartphone at 30 fps video recording.

652

653 Smartphones can also serve as platforms for surface plasmon resonance (SPR)-based assays.

654 Preechaburana *et al.* designed a disposable device that used a smartphone (iPhone 4) display

655 screen as a light source and used its user-facing camera to measure reflectivity.[123] The SPR

656 coupler was made from polydimethylsiloxane (PDMS) and epoxy to gently adhere to the phone's

657 screen, which in turn displayed a guide for alignment with a red rectangle that provided

658 illumination. Image acquisition was done using a custom app that allowed for control of

659   exposure time and ISO number (*i.e.*, sensitivity level to light). This platform was able to detect

660   β_2 microglobulin (β_2M), a biomarker for cancer, kidney disease and inflammatory disease, over a

661   clinically relevant range of concentrations with an LOD of $0.1\ \mu g\ mL^{-1}$.

662

663   In addition to cell phones and smartphones, CMOS-based digital imaging assays run the gamut

664   of technology from conventional digital cameras to new wearable devices. For example, Deiss *et*

665   *al.* recently developed low-cost, portable paper-based culture devices for the analysis of

666   antimicrobial susceptibility using a digital photography camera (Canon EOS Rebel T3i) for

667   readout,[124] whereas the Ozcan Laboratory demonstrated the use of Google Glass for readout of

668   LFS immunoassay results, identification of sample codes, and transmission, analysis and storage

669   of the results using hands-free voice operation.[100]

670

671   Many of the CMOS-imaging assays that are being developed utilize a growing array of NP

672   materials. To date, the most common materials include Au NPs for colourimetric detection, as

673   was the case for the Google Glass example noted above, as well as QDs and UCNPs for

674   fluorescence detection. Several examples of assays that utilize consumer CMOS-imaging devices

675   for readout of NP labels are described in the following sections.

676

677   **3.2.3 Assays with Au NPs**

678   Recently, the Erickson Laboratory developed a competitive direct-antigen immunoassay for the

679   detection of vitamin D with smartphone (Apple iPhone) readout.[125] Serum concentrations of 25-

680   hydroxyvitamin D ($25(OH)D_3$) are routinely used in clinical settings to evaluate vitamin D

681   deficiency (< 50 nM). A $25(OH)D_3$ derivative was immobilized on a solid substrate and Au NP

682   conjugates of anti-$25(OH)D_3$ antibodies were added to serum-extracted samples on this substrate

683   (Figure 7). Competitive binding of antibody between the immobilized $25(OH)D_3$ derivative and

684   the $25(OH)D_3$ native to the serum sample determined the number of Au NPs bound to the

685   substrate. After 6 h of incubation and subsequent silver enhancement, detection and reference

686   areas on the substrate were imaged with the smartphone, where the relative brightness of these

687   areas in images was used for quantitation and accounted for variations in exposure time between

688   different measurements. Assay results showed good correlation with a standard ELISA assay.[125]

689   Lu *et al.* demonstrated the detection of human IgG with silver-enhancement of Au NPs within

690   microfluidic channels.[126] The microfluidic chip was assembled with a polystyrene substrate

691   suitable for the adsorption of antibodies and a PDMS top layer with embedded channels. Post-

692   assay images were acquired with a cell phone camera (Sony-Ericsson K790C) and converted to

693   8-bit grayscale images with computer software. Mean pixel values within the immunoassay

694   zones were used for quantitation of human IgG over the range 0–4 ng mL^{-1}.[126]

695
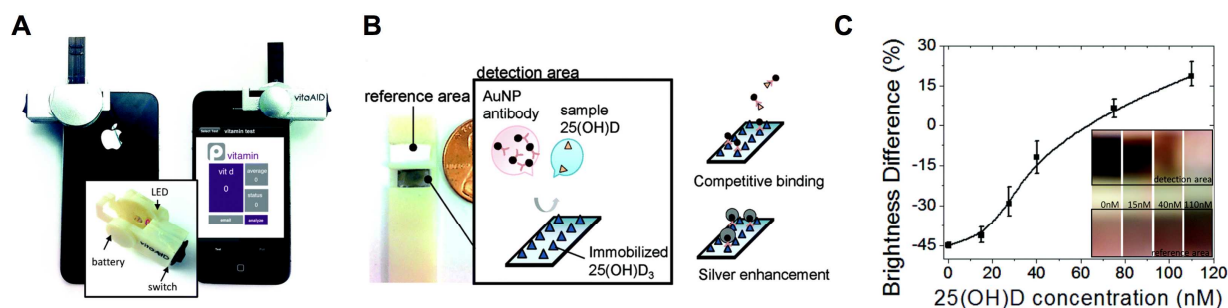
696

697   **Figure 7.** Smartphone-based assay for vitamin D. **(A)** Photograph of an iPhone fitted with an attachment
698   used to acquire colour images as part of a competitive immunoassay for detection of vitamin D. **(B)**
699   Competitive immunoassay format and silver enhancement for signal amplification. **(C)** Data was analysed
700   as an intensity difference between a detection area and a reference area. The inset shows representative
701   colour images after silver enhancement. Adapted from ref.[125] with permission from The Royal Society of
702   Chemistry.

703

704   In addition to silver enhancement of Au NPs, gold enhancement of Au NPs is a means of signal

705   amplification. An example of this procedure is described in Section 3.3.2; however, an

706   interesting variation was reported by the Brennan Laboratory as part of a colourimetric assay for

707   the detection of paraoxon, a neurotoxic agent associated with parathion, a potent pesticide.[127] A

708   paper test strip was modified with a sol-gel with co-entrapped Au NP seeds (3 nm) and

709   acetylcholine esterase (AChE). Samples for paraoxon detection were spiked with a Au(III) salt

710   and acetylcholine. In the absence of paraoxon, the turnover of acetylcholine by AChE produced

711   thiocholine, which then reduced the Au(III), resulting in growth of the seed Au NPs and

712   evolution of the characteristic deeper red colour of larger Au NPs. As an AChE-inhibitor,

713   increasing amounts of paraoxon between 0.5 µM–1 mM slowed this process, resulting in a less

714   colour change, the intensity of which was quantified from analysis of digital camera images.

715

716   As an alternative to silver enhancement, Choi *et al.* achieved up to 100-fold signal amplification

717   by using a two-step detection method with two sizes of Au NP in a LFA for troponin I with

718   digital imaging readout.[128] Initially, Au NPs conjugated with both anti-troponin I antibody and

719   bovine serum albumin (BSA) were used as reporters that bound to analyte captured in the test

720   zone. Subsequently, Au NPs conjugated with anti-BSA antibodies bound to the first set of

721   reporters and were retained in the test zone. Staggered delivery of these two reporters was

722   achieved by staggering their starting positions on the LFS. LFA results were obtained from

723   digital camera images that were processed in software to extract colour intensities of the test

724   lines, or with a sophisticated automated strip reader system (see Section 3.5.1 for strip reader

725   assays). The size of the Au NP in each reporter conjugate was an important determinant of

726   sensitivity, where optimum results (LOD of 0.01 ng mL^{-1} in 10 min) were obtained for 10 nm Au

727   NPs with anti-troponin I and 40 nm Au NPs with anti-BSA (Figure 8). The method was suitable

728   for assaying troponin I in patient serum samples over the range 0.10–14.27 ng mL^{-1}, where the

729   cut-off value for the diagnosis of myocardial infarction is 0.1 ng mL^{-1}.

730
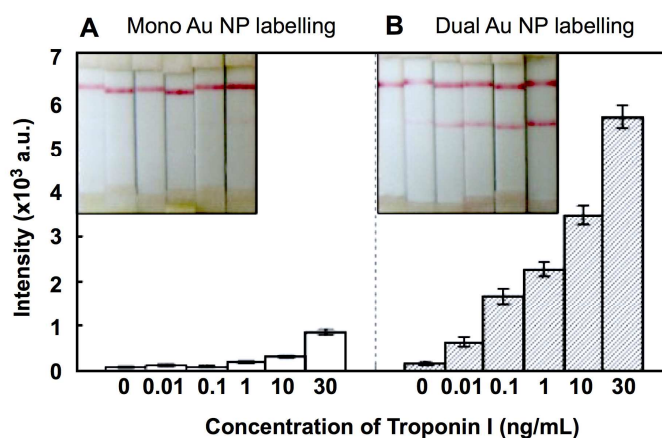
731

732   **Figure 8.** Lateral flow immunoassay for the detection of troponin I. **(A)** Conventional detection format with

733   Au NP (10 nm)-antibody conjugates. **(B)** Enhancement of the sensitivity of the assay by using a two-step

734   method with two different sizes of Au NP (10 nm and 40 nm). Adapted with permission from ref.[128]

735   Copyright 2010 Elsevier.

736

737   Yet another approach to improving the sensitivity of a LFA was taken by Chiu *et al.*,[129] who

738   designed a multilayered paper well for delivery of sample to a LFS with pre-concentration of

739   analyte. The conventional sample pad was replaced with this well (a stack of nine 8×10 mm^2

740   laser-cut strips of fibre glass) and the sample was added as part of a mixed aqueous two-phase

741   system (ATP).[129] Phase separation occurred as the ATP solution flowed through the well,

742　resulting in pre-concentration of the analyte in the leading, smaller-volume phase with a 10-fold

743　improvement in the LOD for immunochromatographic detection of transferrin. Dextran-coated

744　Au NPs conjugated with anti-transferrin antibodies were used as reporters, with readout from

745　digital camera images (Canon EOS 1000D) after a 10 min assay time.

746

747

748　**3.2.4　Quantum Dots**

749　Among fluorescent NP materials, QDs are among the best suited for POC/PON assay formats. In

750　addition to their aforementioned brightness (see Section 2.5), the spectrally broad absorption of

751　QDs permits the straightforward use of relatively broadband excitation sources (e.g., LEDs)

752　without high background in emission measurements. One of the earliest studies to recognize

753　these advantages was by Sapsford *et al.,* who built a microchip detection platform for QD-based

754　assays with an electroluminescent strip light source and a cooled CCD camera for measurement

755　of QD PL.[130] Cell phones and smartphones, which have many advantages over CCD cameras

756　(including cost), have since been used for readout of QD PL in assays with LED excitation

757　sources. The Ozcan Laboratory utilized QDs as fluorescent labels for the detection of

758　*Escherichia coli* O157:7 (*E. coli*) using cell phone imaging (Sony Ericsson U10i Aino).[131] The

759　inner surface of glass capillaries was used as a solid support for the immobilization of anti-*E.*

760　*coli* antibodies. The capillaries were placed in a custom-built cell phone attachment that

761　accommodated two sets of UV LEDs for excitation of the red-emitting QDs and a suitable

762　longpass filter to isolate QD emission (Figure 9). *E. coli* were detected in a sandwich

763　immunoassay with biotinylated secondary antibody and streptavidin-coated QDs. The LOD in

764　buffer and milk samples was *ca.* 5–10 CFU mL^{-1} with good specificity.

765

766

767
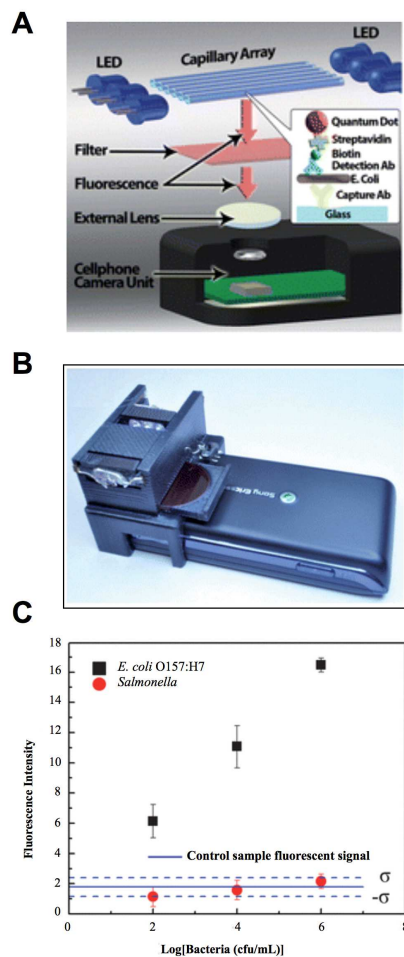
Figure 9. Smartphone-based detection of *E. coli* using QDs as labels in a sandwich immunoassay. **(A)** Schematic and **(B)** photograph of a cell phone fitted with an attachment for fluorescence detection. The attachment housed LED excitation sources, a longpass filter, and a lens to image a parallel array of 10 capillary tubes that were modified with capture antibodies for the immunoassay. (C) The specificity of immunoassay for *E.coli* O157:H7 was demonstrated against *Salmonella* contaminated samples. Adapted from ref.[131] with permission from The Royal Society of Chemistry.

774

Another advantage of QDs is their spectrally narrow emission, which permits direct use of the built-in colour filters of CMOS image sensors for ratiometric detection and spectral multiplexing. Ratiometric detection is ideal for POC/PON applications because of its relative insensitivity to variations in excitation intensity and emission detection efficiency, which may be inherent to low-cost components, battery operation, and inconsistencies in the distance and relative orientation between the light source, sample and CMOS sensor. The Algar Laboratory demonstrated Förster resonance energy transfer (FRET) assays with QDs and smartphone imaging, including heterogeneous paper-based assays with array-based multiplexing[132] and

783   homogenous assays with spectral multiplexing.[133] Both assays utilized trypsin, chymotrypsin,

784   and enterokinase as model analytes for assaying proteolytic activity. In the heterogeneous assay

785   format,[132] green-emitting CdSeS/ZnS QDs were immobilized on a paper substrate and

786   conjugated with Alexa Fluor 555 (A555)-labelled peptide substrates with recognition sites for the

787   proteases of interest. The QD and A555 formed a donor-acceptor pair for FRET, where, upon

788   excitation with a violet LED, QD and A555 emission were measured in the green and red

789   channels of images acquired with a CMOS image sensor (see Figure 10A). Disruption of FRET

790   by proteolytic activity was tracked by changes in the ratio of red/green channel intensities.

791   Consistent results were obtained between a low-cost digital camera (Moticam 1), an off-the-shelf

792   webcam (Logitech C270), and a smartphone (iPhone 4S). Use of these CMOS devices was

793   facilitated by enhancement of FRET within the paper matrix,[134] in addition to the brightness and

794   spectrally narrow emission of the QDs, the latter of which permitted measurement of A555

795   emission in the red channel without crosstalk from QD emission. In the homogenous assay

796   format,[133] all three colour channels of a smartphone camera were utilized by matching the

797   channels to QDs that had emission in the blue, green and red regions of the spectrum (Figure

798   10B).[133] The narrow emission of the QDs minimized crosstalk. Three-plex assays for proteolytic

799   activity were demonstrated by forming FRET pairs between the blue-, green- and red-emitting

800   QDs and QSY35 quencher, QSY9 quencher and Alexa Fluor 647, respectively. Samples in clear-

801   bottomed microtiter plate wells were illuminated with a battery-powered UVA lamp (4 W) and

802   time-lapse images were acquired with a smartphone app. The rate of change in the intensity of

803   each RGB channel was correlated with a particular protease concentration, where it was possible

804   to detect less than 20 pM of protease under optimum conditions.

805
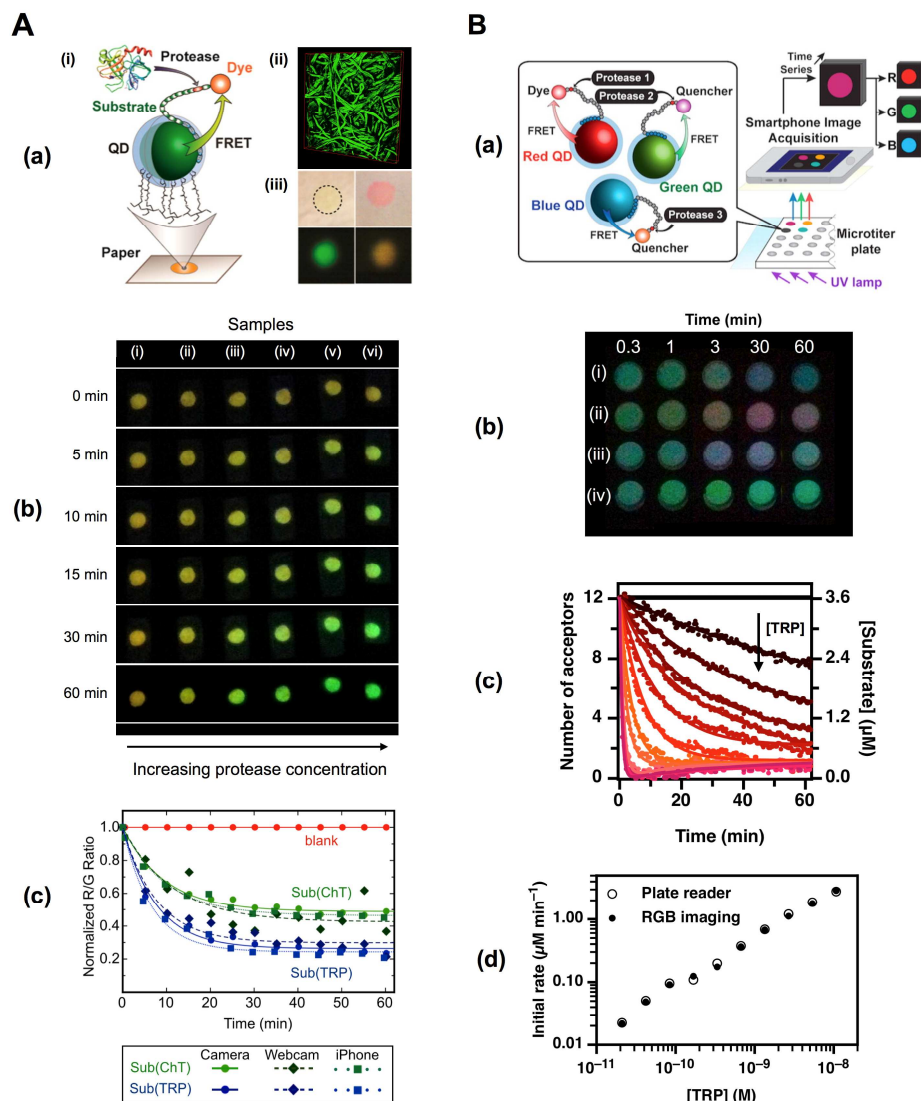
806
807 **Figure 10. (A)** Paper-based, ratiometric QD-FRET assay for the detection of protease activity. (i) Assay
808 format: (a) Immobilized QDs conjugated with dye-labelled peptide substrates on a paper test strip;
809 (ii) confocal PL image of QDs immobilized on cellulose paper fibres; (iii) photographs of paper substrates
810 modified with QDs (left) and QD-peptide-dye conjugates (right), taken under white light (top) and UVA
811 illumination (bottom). (b) Time-lapse images of changes in test strip PL with different concentrations of
812 protease solution (i-vi). Test strip PL changes from yellow to green with loss of FRET. Images were
813 recorded with a smartphone camera under violet LED illumination. (c) The red/green (R/G) ratio from
814 those images permits quantitative tracking of proteolysis. Comparable results were obtained between a
815 digital camera, webcam and smartphone. Adapted with permission from ref.[132] Copyright 2013 American
816 Chemical Society. **(B)** Multiplexed homogeneous assay for protease activity with QDs and FRET.
817 (a) Schematic of the assay design. (b) Colour images of blue-, green- and red-emitting QD-peptide
818 conjugates with exposure to different amounts of three proteases (i-iv). (c) Progress curves for different
819 concentrations of a protease obtained from RGB image readout. (d) Comparison of initial proteolytic rates
820 for replicate assays with smartphone (RGB imaging) readout *versus* a conventional fluorescence plate
821 reader. Adapted with permission from ref.[133] Copyright 2013 American Chemical Society.
822

823　In the above examples, QDs excelled in readout configurations where most fluorescent dyes

824　would have fared poorly: the spectrally narrow absorption band and small Stokes shift of dyes is

825　not ideal for unmodified excitation from an LED, nor is their typically lower brightness, and

826　their spectrally broader emission would generate crosstalk between the RGB colour channels in

827　smartphone images.

828

829　**3.2.5 Phosphorescent NPs**

830　Juntunen *et al.* evaluated polystyrene NPs carrying phosphorescent europium(III) chelates as

831　labels for the LFA detection of prostate specific antigen (PSA) and streptavidin-biotin

832　interactions, and compared these two model assays to analogous Au NP-LFA assays.[135] The

833　phosphorescence-based assays exhibited between 7–300-fold greater sensitivity than the Au NP

834　labels, albeit with the caveat of using different readout systems. Phosphorescence imaging was

835　done with UV lamp (6 W) excitation and a digital camera (Canon PowerShot SX130; 15 s

836　exposure time) with a suitable bandpass filter, whereas optical density measurements for Au NP

837　LFAs were done with a flatbed scanner (CanoScan 9900F; see Section 3.3 for scanner-based

838　assays). The digital camera imaging of phosphorescent NPs was also compared with

839　measurements using a filter-based plate reader system equipped with a xenon lamp and PMT

840　detector (PerkinElmer Victor X4). Given that europium chelates have emission lifetimes on the

841　order of 10^{-4} s, both prompt emission and time-gated emission measurements were possible with

842　the plate reader. The advantage of time-gating is the ability to reject short-lived ($< 10^{-6}$ s)

843　background from assay substrates or sample matrices. Unsurprisingly, the time-gated plate

844　reader measurements with phosphorescent NP labels provided the lowest LOD (0.02 ng mL^{-1}

845　streptavidin), followed by non-time-gated plate reader measurements (0.03 ng mL^{-1}) and digital

846　camera imaging (2.2 ng mL^{-1}). The Au NP LFA had the least favourable LOD (6.1 ng mL^{-1}).

847

848　**3.3 Scanners**

849　**3.3.1 Technology**

850　Scanners can create digital images with a large field of view (> 600 cm^2), good resolution (≥ 600

851　dpi), and a wide range of optical density (0–4). Imaging is done with either CCD sensor or

852　contact image sensor (CIS) technologies (Figure 11). CCD-based scanners are equipped with

853　white light illumination and a demagnifying lens to focus the entire field of view onto the image

854   sensor, which comprises three linear arrays of CCD elements sensitive to red, green and blue

855   light. The CIS image sensor is a linear array of photodiodes that is located next to the bottom

856   surface of the glass imaging surface. The illumination system is a combination of red, green and

857   blue LEDs, which avoids the need for optical filters. Although this configuration does not require

858   demagnification, it has a much shorter depth of field (*ca.* 100 µm) than CCD sensors. CIS-based

859   scanners have become a *de facto* standard for most office and consumer settings because of their

860   smaller size, greater robustness, lower cost, and lower power consumption when compared to

861   CCD-based scanners.

862

863   The flatbed scanner was one of the first consumer electronic devices to be used for the readout of

864   bioassays. Scanners have been extensively utilized for quantification of LFAs with Au NP labels,

865   both without[136-140] and with[141, 142] silver staining, as well as assays with colloidal carbon NPs[143-

866   146] and viral NPs[147] labels. Examples of these assays are described below.

867

868
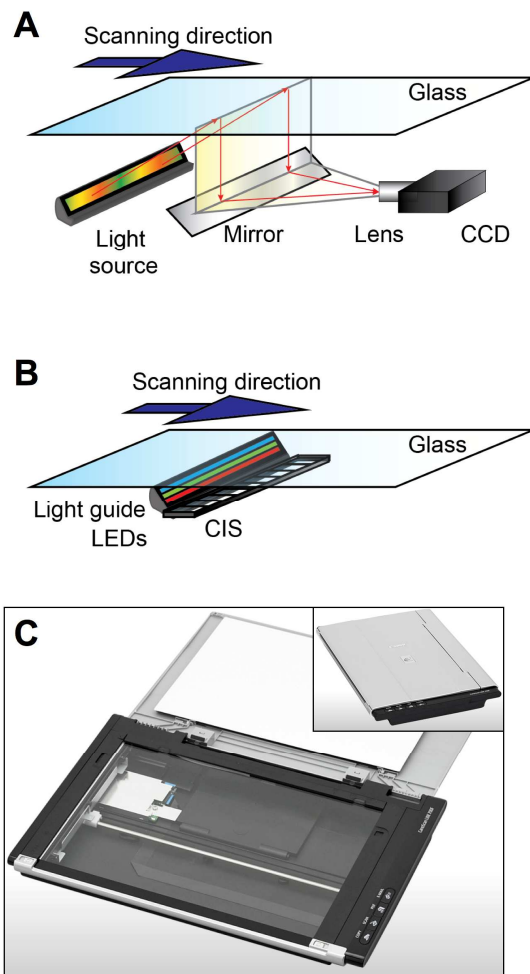
Figure 11. Simplified schematic of the main optical components in **(A)** CCD and **(B)** CIS scanners. **(C)** Example of commercially available USB-operated scanner (Canon CanoScan LiDE 700f).

871

3.3.2 Au NPs

Increasing amounts of Au NPs and silver-enhanced Au NPs appear progressively darker in grayscale images from scanners. Although this readout platform remains popular after more than a decade, there are indications its use will diminish with increased use of smartphone imaging.

876

Recently, Warren *et al.* developed a detection platform for non-communicable diseases (*e.g.*, stroke, heart disease, cancer) using synthetic biomarkers for enzyme activity and LFA-based urinalysis with scanner readout.[136] Protease-sensitive NPs were constructed by conjugating peptide substrate-biotinylated ligand chimeras to iron oxide nanoworms known to have long circulation times *in vivo*. Following injection into mice, hydrolysis of peptide substrates by

882   upregulated proteases released the biotinylated ligands *in vivo* with subsequent excretion in

883   urine. Urine was analyzed with a LFIA that had anti-ligand capture antibodies and used Au NP-

884   streptavidin conjugates as reporters, allowing for multiplexed detection of proteolytic activity

885   associated with thrombosis (thrombin) and colorectal cancer (matrix metalloproteinase-9), as

886   shown in Figure 12. To account for the variations in analyte concentration in urine due to host

887   and environmental factors, the authors also included an internal standard in their assay.

888   Quantitative analysis of LFIA results from scanned images (Epson V330 Photo scanner)

889   provided an LOD of 1 nM with a dynamic range of 1–7 nM. The authors also noted a good

890   correlation between scanner images and smartphone images (Samsung Galaxy Nexus).[136]

891
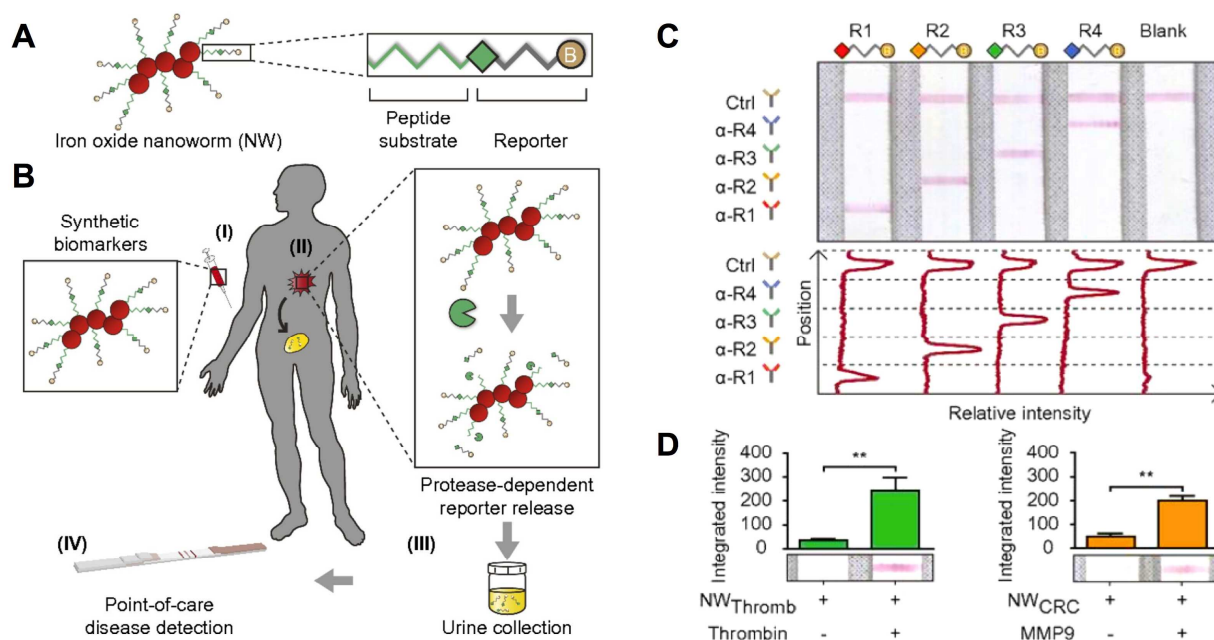
892

893   **Figure 12.** Assay for cancer biomarkers with protease-sensitive iron oxide nanoworms (NWs).
894   **(A)** Nanoworms are conjugated with peptide substrates for thrombin and matrix metalloproteinase-9
895   (MMP9). **(B)** The nanoworms are administered through (i) intravenous injection to (ii) measure proteolytic
896   activity *in vivo*. Reporters released by proteolytic activity are (iii) excreted in urine and analysed by (iv)
897   LFIA. **(C)** Spatially multiplexed LFIA to detect reporters spiked in mouse urine. The positions of
898   immobilized capture antibodies are indicated. **(D)** *In vitro* assays for thrombin (left) and MMP9 (right) in
899   spiked mouse urine samples. The graphs show the test line intensities without (–) and with (+) protease.
900   Full assays depicted in panel B were done with mouse models. Adapted from ref.[136] Copyright 2014 the
901   original authors.

902

903

904   Some other notable examples of scanometric LFAs with Au NP reporters include work by Gong

905   *et al.* on a "lab-in-a-pen" device that contained a lancet for direct drawing of blood from a finger

906   prick and clinical detection of Hepatitis B biomarkers,[137] and LFAs demonstrated by Anfossi *et*

907   *al.* for the detection of fumonisins[139] and aflatoxins[140] in corn and cereal samples, using portable

908   USB-powered scanners (CanoScan LiDE 200 and OpticSlim 500). The Juncker Laboratory has

909   also reported the use of a USB-scanner (CanoScan LiDE 700; Figure 10C) for readout of Au NP-

910   based immunochromatographic assays developed on cotton thread rather than a conventional

911   LFS.[138] C-reactive protein (CRP), a cardiac biomarker, was detected in buffer and serum with an

912   LOD of *ca.* 10 ng mL^{-1}, where the clinically relevant cut-off for CRP detection is 3 μg mL^{-}

913   ^{1}.Multiplexed detection of CRP, leptin, and osteopontin within 20 min was also demonstrated

914   with the thread format and scanometric readout.[138]

915

916   Similar to smartphone imaging, the detection of low-abundance analytes with Au NPs and a

917   scanner may require a signal amplification strategy such as silver enhancement. Such was the

918   approach in a LFA for detection of amplified HIV-1 RNA for assessment of viral load.[141] In this

919   study by Rohrman *et al.*, Au NP-oligonucleotide conjugates were used as reporters and an

920   extensive range of parameters were optimized, including Au NPs size (50–60 nm was optimal

921   from a 15–80 nm range). Interestingly, the authors found that gold enhancement of Au NPs

922   provided a larger improvement in signal-to-noise ratio than silver enhancement (25% *vs.* 15%)

923   by providing lower background. Under optimum conditions, and using scanner imaging (Epson

924   Perfection V500 Photo scanner) for readout, the LOD for plasmid RNA was 9.5 log$_{10}$ copies

925   with a linear dynamic range from 10.5 log$_{10}$–13 log$_{10}$ copies.[141] Similarly, the Yu Laboratory has

926   utilized silver enhancement for scanometric assays with hairpin oligonucleotide probes

927   immobilized on polycarbonate substrates.[142] In this format, one terminus of a hairpin probe was

928   attached to the substrate while the other was biotinylated but inaccessible to streptavidin due to

929   its proximity to the substrate surface. Depending on its sequence and design, the hairpin probe

930   opened in response to a target DNA sequence, thrombin, or Hg^{2+} ions. Au NP-streptavidin

931   conjugates then bound to the distal biotin, were silver enhanced, and read out as grayscale

932   intensities using a scanner (Microtek). Detection limits for the three targets were between 1–10

933   nM.[142]

934

3.3.3 Colloidal Carbon NPs

Amorphous carbon black NPs are easily synthesized, inexpensive materials that offer high contrast for imaging LFAs on white paper. A major challenge with this NP is its high tendency for aggregation, particularly during the drying step needed for preparation of the conjugate pad of a LFA. Nevertheless, LFS immunoassays have been demonstrated for detection of erythropoietin,[143] a glycoprotein hormone that regulates production of red blood cells. The LFS were imaged using a scanner (Epson) set to produce in 16-bit grayscale images that were analyzed in software. The LOD was 1.2 fM, which was two orders of magnitude lower than the corresponding ELISA.[143] In another LFA, methiocarb pesticide in surface water was detectable down to 0.5 ng mL^{-1} within 10 min using 120 nm amorphous carbon NP-antibody conjugates.[144] The LFS were scanned in grayscale mode (Epson Perfection V700 Photo scanner) and the test line intensities were analyzed in software. Scanner readout was also used for the detection of carbohydrate-deficient isoforms of transferrin with a LFS that incorporated affinity- or ion-exchange-based removal of unwanted isoforms prior to immunochromatographic detection with colloidal carbon-antibody conjugates as reporters.[145]

Linares *et al.* designed model dot blot assays with biotin-streptavidin binding to compare the performance of Au NPs, silver-enhanced Au NPs, blue latex beads, and carbon NPs.[146] The carbon NPs provided the best LOD (0.01 μg mL^{-1}), followed by silver-enhanced Au NPs (0.1 μg mL^{-1}), Au NPs (1.0 μg mL^{-1}), and latex beads (1.0 mg mL^{-1}). Dot blots were scanned (Hewlett-Packard 3800 Scanjet) and the images processed in software by splitting into RGB colour channels. The channel with the most intensity was converted into an 8-bit grayscale image for quantification. Although carbon NPs significantly improved assay sensitivity, these materials have limited colloidal stability and lack of functional groups on the surface, the latter of which stipulates the preparation of bioconjugates through non-specific adsorption. A drawback of this approach is that it does not permit control over the orientation of antibodies, which can result in non-trivial loss of binding activity.[79]

3.3.4 Viral NPs

Although the major focus of research on VNPs is their use as delivery vehicles for drugs and contrast agents,[148] VNPs have also been utilized as carriers for labels in assays. Adhikari *et al.*

36

966   designed a LFA-ELISA for the detection of MS2 bacteriophage using bacteriophage M13 VNPs

967   that were modified with horseradish peroxidase (HRP) and target-specific antibodies.[147]

968   Quantification of MS2 relied on the generation of blue colour with turnover of 3,3′,5,5′-

969   tetramethylbenzidine (TMB) by HRP. An LOD of 10^4 pfu mL^{-1} was possible with scanner

970   readout (Epson V600 color scanner) and image analysis in software. This LOD was 1000-fold

971   better than the LOD for an LFA with Au NP labels.

972

3.4 Optical Disc Drives

3.4.1 Technology

975   Optical disc drives, colloquially known as CD, DVD and Blu-Ray Disc (BRD) players and

976   writers, read information using a diode laser and photodiode. With the aid of a tracking drive and

977   a disc drive, the laser beam scans the surface of the disc in a spiral pattern, from the centre

978   outwards, as the disc spins. Discs comprise a polymer substrate with tracks of "pits" and "lands"

979   coated with a reflective layer of metal and an additional layer of polycarbonate. The laser beam

980   is reflected from lands and detected by the photodiode (Figure 13A) resulting in a digital 1 bit.

981   Laser light reflected from pits does not reach the photodiode and generates a digital 0 bit. The

982   primary difference between CD, DVD, and BRD players is the wavelength of the laser used and

983   the consequences it has on the storage capacities of the corresponding discs. CD drives use near-

984   infrared lasers (780 nm), DVD drives use red lasers (650 nm), and BRD drives use violet (405

985   nm) lasers. Shorter wavelengths of light can be focused to a smaller diameter spot, permitting

986   greater resolution and use of smaller pits and lands for higher data densities. The primary

987   mechanical components (Figure 13B) are standard between the different drive types.

988
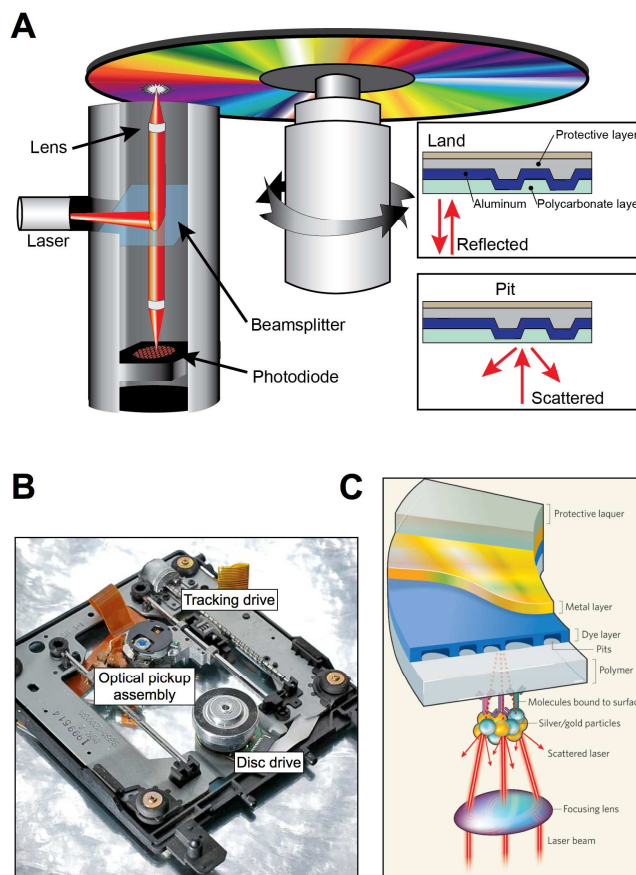
Figure 13. (A) Simple schematic illustrating readout of a CD/DVD/BRD in an optical drive. **(B)** Photograph of the primary mechanical components of an optical drive (adapted from Wikipedia). **(C)** Readout principle of binding assay on a disc: Au NPs bound to the disc through selective binding events are silver enhanced to form larger particles that scatter the laser beam, which alters the digital readout of the disc. Panel C reprinted with permission from ref.[149] Copyright Macmillan Publishers Ltd: Nature 2008.

As recently reviewed,[150, 151] the use of CDs/DVDs for centrifugal microfluidics has been an active area of research for many years. Despite significant progress in the field, particularly with respect to biomedical diagnostics, there are only a few commercialized products. One example is a commercial centrifugal device developed by Abaxis that requires only a 100 µL blood sample to perform a range of medical tests in a multiplexed format, including measurement of important electrolytes and metabolites, and biomarkers for hepatic, renal, and liver function.[152] The data is acquired with a special readout instrument that acts as a spectrophotometer, incorporating a xenon flash lamp, optics, and photodetector for absorbance measurements of colourimetric

1005　indicators at nine different wavelengths. Despite the convenience and sample-to-answer assay

1006　format, the instrument cost ($16 500) and the cost of test cartridges ($30-40 each) remains a

1007　potential barrier to widespread use, particularly in low-resource settings.

1008

1009　Digital discs are inexpensive, and their polycarbonate surface can be exploited as a substrate for

1010　array-based assays through simple surface chemistry modifications using UV/ozone treatment[153]

1011　or through physisorption without pretreatment.[154] The readout of disc-based assays can be done

1012　with custom hardware modifications of commercial optical drives,[155] or with off-the-shelf

1013　CD/DVD/BRD players or computer optical drives. For POC/PON applications, off-the-shelf

1014　units are much more accessible and cost effective. For readout, objects with a size greater than

1015　one-quarter the laser wavelength can disrupt its reflection (Figure 13C), and the Yu Laboratory

1016　has found that these disruptions can be converted into quantitative information by running freely

1017　available disc-diagnostic software.[29] The error distribution trends are reproducible between

1018　different software programs and different optical drives.[156] An alternative approach for readout,

1019　described by the Maquieira Laboratory, extracts binary code from the disc using custom

1020　hardware and software.[157, 158] Signals from the disc player photodetector are digitized and

1021　deconvolved into an image, where the image optical density is proportional to analyte

1022　concentration.[157, 159]

1023

1024　**3.4.2　Au NPs**

1025　The abovementioned readout strategies for CD/DVD drive assays have been used to monitor

1026　streptavidin-biotin binding,[160] for DNA hybridization assays[156] and immunoassays,[157, 161] and for

1027　assaying metal ions.[162] Recently, BRD optical drives have also been used for readout of biotin-

1028　streptavidin interactions,[163] competitive immunoassays and DNA hybridization assays.[154, 164]

1029　Silver-enhanced Au NPs were used as reporters in each of the foregoing assays because

1030　disruption of the laser beam during disc scanning occurs to a greater extent with larger objects.

1031　For example, the Yu Laboratory demonstrated CD-based DNA hybridization assays and

1032　immunoassays for human IgG (see Figure 13) with LODs of 25 nM and 25 ng mL^{-1},

1033　respectively.[156] Most recently, these researchers reported a quantitative disc-based assay with

1034　performance comparable to a standard ELISA using human chorionic gonadotropin (hCG) as a

1035　model biomarker (Figure 14).[164] A DVD was modified with a multichannel PDMS plate, and

1036   sandwich assays were done in the channels with Au NPs as reporters. Following silver

1037   enhancement, hCG concentrations were determined from readout in terms of error distributions

1038   (PIF) obtained from an optical drive and disc quality software, or from readout in terms of

1039   optical darkness ratio (ODR) obtained from scanner images (Epson Perfection 1250). The 1.5

1040   mIU mL^{-1} LOD was comparable to a standard ELISA test, and there was good correlation

1041   between disc assay results and ELISA results for urine samples from pregnant women.[164] The

1042   Maquieira Laboratory has demonstrated a DVD-based assay for multiplexed detection of

1043   atrazine, chlorpyrifos, metolachlor, sulfathiazole, and tetracycline with LODs in the range 0.10–

1044   0.37 µg L^{-1} and dynamic ranges over two orders of magnitude.[157] These researchers also

1045   developed a BRD-based assay for microcystine LR, a naturally occurring toxin, with an LOD of

1046   0.4 µg L^{-1}, a dynamic range between 0.12–2.00 µg L^{-1}, and a total assay time of 60 min.[154]

1047
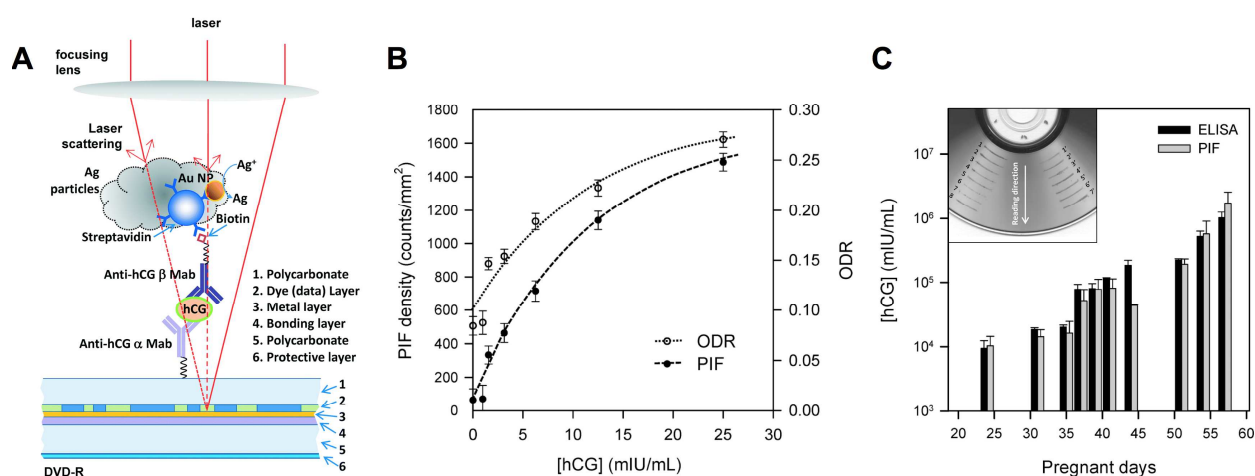
1048

1049   **Figure 14.** DVD-based assay for hCG: **(A)** Illustration of the assay format and scatter of the laser beam
1050   by silver-enhanced Au NPs; **(B)** calibration curve for hCG in terms of disc error distribution (PIF; optical
1051   drive readout) and optical darkness ratio (ODR; scanner readout); **(C)** Comparison of urine hCG levels
1052   measured with the DVD-based assay and a standard ELISA for a pregnant woman. The inset in panel C
1053   shows a photograph of the DVD with PDMS sample channels. Adapted from ref.[164] with permission from
1054   The Royal Society of Chemistry.

1055
1056

1057   To the best of our knowledge, silver-enhanced Au NPs are the only NP materials to have been

1058   used as a reporter for optical disc-based assays to date. Among the other NP materials discussed

1059   in this review, carbon black NPs would presumably be the most suitable alternative to metallic

1060   NPs, as they would provide the optical density to modulate reflection of the laser beam used for

1061   readout.

1062

1063   **3.5 Strip Readers**

1064   **3.5.1 Technology**

1065   Strip readers are commercially available or custom-built instruments for readout of LFA strips.

1066   These instruments are either hand-held or have a small bench-top footprint, as shown in Figure

1067   15. Although not mainstream consumer devices, they are designed with the intention of being

1068   retailed at relatively low cost and with wide distribution, and their operation is conceptually

1069   similar to those for scanners and CMOS camera devices. Light sources for optical readout are

1070   typically white light LEDs for readout of colourimetric labels such as Au NPs, coloured latex

1071   NPs, and carbon NPs; coloured LEDs or laser diodes for fluorescent dyes and QDs; or low-

1072   power NIR lasers (~1 W)[165] for UCNPs. There are several commercial manufacturers of strip

1073   readers (*e.g.*, Qiagen, Scannex, LRE, BD Diagnostics, Unison Biotech, and many others) with

1074   prices ranging from a few hundred dollars to a few thousand dollars.

1075
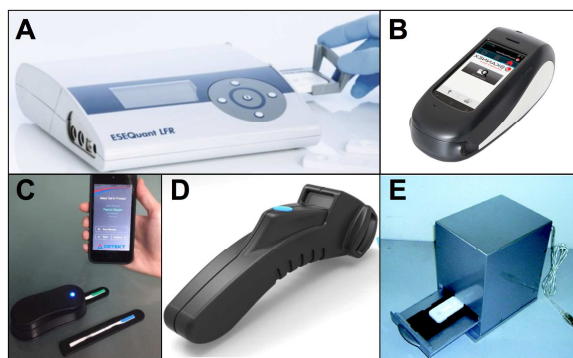
1076

1077   **Figure 15.** Examples of commercial strip readers from **(A)** Qiagen (ESE Quant), **(B)** Scannex,
1078   **(C)** iDetect, **(D)** DCN Diagnostics, and **(E)** Shanghai Kinbio Tech (DT1030).
1079

1080   **3.5.2 Au NPs**

1081   The value of Au NPs as reporters in strip reader assays is analogous to their value in scanometric

1082   and disc-based assays: the Au NPs provide a high degree of optical contrast through modulation

1083   of reflected light intensity. As with the other assay formats, silver enhancement can improve

1084   assay sensitivity; however, an alternative strategy with similar gains has been demonstrated in

1085   strip reader assays. This alternative strategy entails the use of nanocomposite labels that have

1086   many Au NPs attached to a larger NP scaffold, effectively increasing the net extinction

1087   coefficient per label. As an example, Xu *et al.* recently demonstrated improved sensitivity for

1088   LFIAs with Au NP-decorated silica nanorods as labels for the detection of rabbit IgG as a model

1089   protein (Figure 16A).[166] The large surface area of the silica nanorods (3.4 μm length, 200 nm

1090   diameter) was modified with both Au NPs (17 nm diameter; final density of ~10^4 per nanorod)

1091   and antibodies (optimum density of ~10^4 per nanorod). The LOD with the Au NP-silica nanorod

1092   composite labels was found to be 0.01 ng mL^{-1}, whereas Au NP labels alone could not detect 1.0

1093   ng mL^{-1} rabbit IgG.

1094
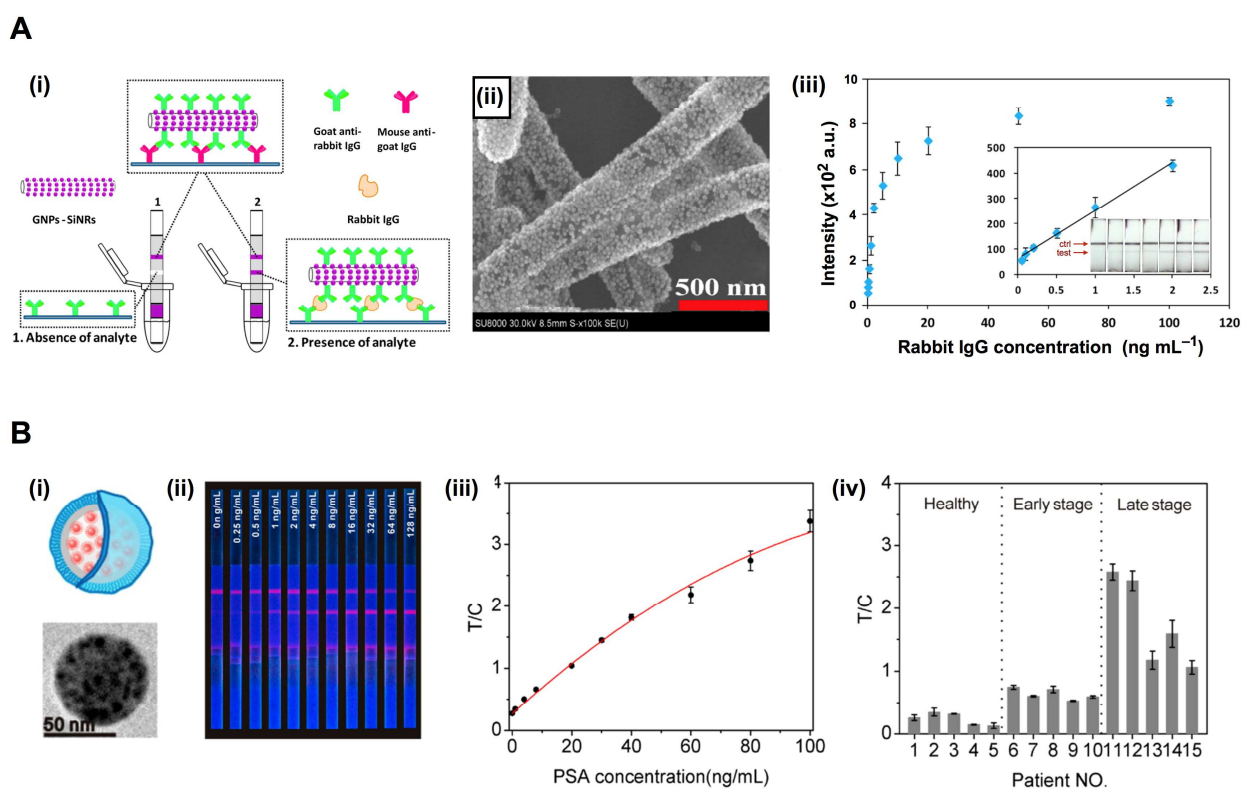
1095

1096   **Figure 16. (A)** LFIA for IgG that uses silica nanorods functionaized with ~10^4 Au NPs for signal
1097   amplification: (i) assay design; (ii) SEM image of the Au NP-modified silica nanorods; (iii) signal from a
1098   strip reader correlates with LFA test line colour intensity. Reprinted with permission from ref.[166] Copyright
1099   2014 American Chemical Society. **(B)** LFIA for prostate specific antigen (PSA) that uses polymer NP-
1100   encapsulated QDs for signal amplification: (i) illustration and SEM image of polymer NP-encapsulated
1101   QDs; (ii) Image of LFSs under UV illumination with visible red PL from the QDs; (iii) calibration curve for
1102   (iv) detection of PSA in clinical serum samples. Reprinted with permission from ref.[167] Copyright 2014
1103   American Chemical Society.

1104

1105   Another method of improving LFA sensitivity with strip readers (Cozart, SpinReact) was

1106   demonstrated by the Merkoçi Laboratory. An array of hydrophobic wax pillars was printed along

1107   a nitrocellulose membrane to produce delays and pseudoturbulence in the microcapillary flow,

1108   yielding three-fold more sensitive detection of HIgG than analogous LFAs without pillars.[168] Au

1109   NP-immunoconjugates were used as reporters.

1110

1111   In addition to LFIAs, Au NPs have been used as reporters in aptamer-based LFAs that use

1112   portable strip readers for readout. Xu *et al.* utilized two thrombin-binding aptamers to construct a

1113   sandwich LFA for thrombin.[169] The test zone of the LFS was modified with streptavidin and

1114   biotinylated primary aptamer, and Au NPs were modified with secondary aptamers. In the

1115   presence of thrombin, Au NPs were retained in the test zone and quantified using a portable strip

1116   reader (DT1030, Shanghai Kinbio Tech). The LOD was 2.5 nM with an assay time of 10 min

1117   and a dynamic range of 5–100 nM. These analytical figures of merit are comparable to LFIAs.

1118   Detection of thrombin in spiked human serum samples was also possible, but with much less

1119   favourable figures of merit (LOD 0.6 µM; dynamic range 1–60 µM).[169] Au NPs have also been

1120   used as reporters in an oligonucleotide-based LFA for Hg^{2+} detection that exploits toehold

1121   binding and Exonuclease III (ExoIII)-assisted signal amplification.[170] A hairpin DNA probe

1122   containing a thymine-thymine (T-T) mismatch in a toehold domain served as a specific

1123   recognition element for Hg^{2+} ions, leading to opening of the hairpin and subsequent ExoIII

1124   activity.[170] A product oligonucleotide fragment was then assayed on a LFS with Au NP-

1125   oligonucleotide conjugates as reporters, permitting indirect detection of Hg^{2+} with a strip reader

1126   (DT1030) and an LOD of 1 pM. For the analysis of environmental water samples, the results

1127   from the LFA agreed with an inductively coupled plasma mass spectrometry assay within

1128 $\leq 7.6\%$. Although the shelf-life of LFS was at least 6 months, the ExoIII enzyme is typically

1129   stored at –20 ℃ and may not be amenable to low-resource or out-of-lab settings.

1130

1131   Undoubtedly, there are many other examples of LFA that use Au NPs as reporters, whether with

1132   strip readers or other readout devices. Indeed, Au NPs have become the label of choice for

1133   LFIAs and are widely used in commercial tests.

1134

1135

1136 **3.5.3 Quantum Dots**

1137 Strip reader assays with QDs are conceptually similar to their smartphone counterparts, where a

1138 LFS is illuminated with excitation light and the QD PL intensity is measured using a

1139 photodetector and an appropriate spectral filter. The drawback of strip readers that do not include

1140 CMOS sensors with a built-in RGB filter is their lack of suitability for spectral multiplexing.

1141

1142 Zou *et al.* have used QD as labels in a LFIA to detect 3,5,6-trichloropyridinol (TCP), a

1143 biomarker for exposure to chlorpyrifos insecticide, in rat plasma.[171] Red-emitting QDs were

1144 conjugated with a TCP derivative, and these QD-TCP conjugates were spotted on the conjugate

1145 pad. Upon LFS development, these conjugates competed with TCP in the sample for binding to

1146 capture antibodies in the test zone. The PL intensity in the test zone was measured with a

1147 portable strip reader (ESE-Quant FLUO). The LOD was 1 ng mL^{-1} (~5 nM) with an assay time

1148 of 15 min.[171] Similarly, Li *et al.* combined a LFA with QD labels for detection of nitrated

1149 ceruloplasmin, an important biomarker for cardiovascular disease, lung cancer, and stress

1150 response to smoking.[172] Yellow-emitting QDs were conjugated with anti-nitrotyrosine and the

1151 test line was modified with polyclonal anti-human ceruloplasmin antibodies. The LOD was 1 ng

1152 mL^{-1} for buffer samples and 8 ng mL^{-1} for spiked human serum samples with a 10 min assay

1153 time. Beyond immunochromatographic LFS assays, Wang *et al.* utilized red-emitting QDs as

1154 reporters in an aptamer-based LFA for the detection of ochratoxin A with an LOD of 1.9 ng mL^{-}

1155 ^{1} and an assay time of 10 min.[173]

1156

1157 Similar to the concept of modifying a larger NP scaffold with many Au NPs, a strategy to

1158 increase the sensitivity of assays with QD reporters is to use a larger polymeric NP as a carrier

1159 for multiple QDs. For example, to improve the sensitivity of a LFIA for prostate specific antigen

1160 (PSA), Li *et al.* encapsulated red-emitting CdSe/CdS/Cd$_x$Zn$_{1-x}$S/ZnS QDs into amphiphilic

1161 triblock copolymer NPs of two different sizes (68 nm or 130 nm diameter).[167] The signal-to-

1162 background ratio was better for the smaller polymer NPs because they exhibited less non-

1163 specific adsorption. The QD-doped polymer NPs (quantum yield 55%, LOD 0.33 ng mL^{-1})

1164 provided a 12-fold better LOD than individual thiocarboxylic acid-coated QDs (quantum yield

1165 38%, LOD 3.87 ng mL^{-1}) and were suitable for assaying clinical serum samples (Figure 16B).

1166 The LOD was sufficient for detection of early-stage prostate cancer where PSA concentrations

1167　are 4–10 ng mL^{-1} (*cf.* normal values of 0.5–2 ng mL^{-1}). In this case, the strip reader was custom

1168　built around a 405 nm diode laser and a fibre-optic spectrometer.[167] In another example, Ren *et*

1169　*al.* developed a LFIA for the detection of aflatoxin B$_1$ (ATB$_1$) in maize using red-emitting

1170　CdSe/ZnS QDs embedded in polymer NPs (230 nm) that were conjugated with anti-ATB$_1$

1171　antibodies.[174] This assay had a dynamic range of 5–60 pg mL^{-1} and an LOD of 0.42 pg mL^{-1}.

1172

1173　**3.5.4　Phosphorescent NPs**

1174　In addition to time-gated measurements (see Section 3.2.5), another approach to minimizing

1175　background fluorescence is use of a NIR light source to excite NaYF$_4$:Yb,Eu UCNPs that emit in

1176　the visible region. Strip readers can meet these specifications. In one example, UCNPs were

1177　conjugated with a monoclonal antibody for the detection of *Vibrio anguillarium*, a pathogen

1178　found in fish.[175] With a 15 min assay time, the LOD was 10^2 CFU mL^{-1}, which was 100-times

1179　better than an ELISA assay for the same target. The dynamic range was 10^3–10^9 CFU mL^{-1}.

1180　UCNP-based assays have been field-tested for diagnostic applications in South Africa[176] and

1181　Ethiopia.[177] Detection of circulating anodic antigen (CAA), a biomarker for *Schistosoma*

1182　infection, was performed on ~2000 clinical serum samples by local physicians in South

1183　Africa.[176] LFA and ELISA results were correlated for CAA concentrations above 300 pg mL^{-1},

1184　and superior performance was noted at lower concentrations (30–90 pg mL^{-1}) for LFAs with a

1185　prototype strip reader (instrument design is described in ref.[165] and was commercialized[178]) and a

1186　commercially available strip reader (ESEQuant). The LFA was also more robust and reliable. A

1187　similar multiplexed LFA with UCNP labels for detection of leoprosy-causing *mycobacterium*

1188　*leprae* was developed by targeting a pro-inflammatory cytokine, IP-10, and anti-PGL-I

1189　antibodies that are indicative of infection.[177] The LFS results correlated with traditional ELISA

1190　results for whole blood assays with Dutch and Ethiopian leprosy patient samples.

1191

1192　In contrast to UCNPs, lanthanide complexes do not exhibit efficient upconversion, and time-

1193　gated measurements are the only option for active background suppression. While such

1194　measurements typically require sophisticated laboratory instrumentation, Song and Knotts

1195　developed a prototype reader for time-resolved LFAs that was simple, portable and low-cost.[179]

1196　These researchers also made use of the nanocomposite label strategy for signal enhancement that

1197　was described for strip reader assays with QDs (see Section 3.5.3). Here, polymer NPs were

1198   doped with either europium(III) complexes, platinum(II) tetra-meso-fluorophenylporphine

1199   (TMPFP) or palladium(II)-TMPFP, and conjugated with a monoclonal antibody for C-reactive

1200   protein (CRP), an inflammatory biomarker. The LOD was < 0.2 ng mL^{-1} in serum with a

1201   dynamic range of 0.2–200 ng mL^{-1}. The reader used an LED with 395 nm emission for pulsed

1202   excitation and silicon photodiodes as detectors: one photodiode was placed at the backing of the

1203   LFS to account for fluctuations in LED intensity; the second photodiode was used to measure

1204   phosphorescence from the NP labels. The total cost of materials for device construction was

1205   approximately $20.[179]

1206

1207   Similar to the above example, the nanocomposite signal enhancement strategy described in

1208   Sections 3.5.2 for strip reader assays with Au NPs can also be utilized with phosphorescent

1209   lanthanide complexes. Song *et al.* used silica NPs loaded with europium(III) chelates as bright

1210   labels for the detection of clenbuterol toxin in urine samples by LFIA.[180] The intensity of the test

1211   line was measured with a strip reader (ESE-Quant LFR), providing an LOD of 0.037 ng mL^{-1}

1212   clenbuterol.

1213

1214

1215   **4. Toward Electrochemical POC Assays with NPs**

1216

1217   Up to this point, we have focused on the role NPs can play in optical POC/PON assays and

1218   diagnostics. Electrochemical assays are also common and versatile formats for chemical and

1219   biological analyses, and many types of NPs have advantageous electrical and electrochemical

1220   properties. However, a key difference between optical and electrochemical readout is that there

1221   are not many consumer devices that are both commonplace and electrochemistry ready—a

1222   notable exception being personal blood glucose meters.

1223

1224   **4.1 Blood Glucose Meters as POC Devices**

1225   Glucose meters are well-established over-the-counter POC devices that allow monitoring of

1226   blood glucose concentration. Typically retailing for $20–$100, personal blood glucose meters are

1227   a multi-billion dollar market,[181] and test strips for those meters are manufactured on the order of

1228 10^{10} per year (reflecting the prevalence of diabetes).[182] Advantages of these devices include low

1229   cost, portability, ease of use and rapid results.

1230

1231   At their core, glucose meters are amperometers that measure turnover of an electron-transfer

1232   mediator in the enzymatic oxidation of glucose, typically by glucose oxidase, but also by glucose

1233   dehydrogenase.[183, 184] The electrical current from the voltammetric conversion of the mediator

1234   back to its initial state is proportional to the concentration of glucose. Measurements require less

1235   than a drop of blood and results are available within seconds. The dynamic range for glucose

1236   detection is typically 0.1–6.0 mg mL^{-1} (0.6–33 mM) glucose. The devices are limited by the

1237   accuracy of the results ($\pm$ 20% is acceptable), which may be subject to errors from batch-to-batch

1238   variation in test strip production, user training and environmental factors.[185]

1239

1240   As an alternative to dedicated blood glucose meter devices, FDA-approved smartphone apps and

1241   plug-in devices have become available.[102, 186, 187] The population affected by diabetes continues

1242   to increase worldwide (387 million worldwide in 2014[188]), with more and more cases of juvenile

1243   diabetes ($\leq$ 20 years of age).[189] Smartphone-based glucose measurements accommodate this

1244   demographic and, more pertinently, highlight that smartphones have diagnostic utility beyond

1245   optical assays.

1246

1247   **4.2 Repurposing Blood Glucose Meters and Cell Phones**

1248   As amperometers, there is no reason that blood glucose meters should be limited to the detection

1249   of glucose; however, assays for non-glucose analytes must be designed to integrate with a device

1250   optimized for only glucose detection. Several strategies have been employed to this end. One

1251   strategy is to replace the glucose oxidase in test strips with other oxidase enzymes; for example,

1252   cholesterol, L-lactate and ethanol have been assayed with blood glucose meters using

1253   ferricyanide as an electron-transfer mediator and cholesterol oxidase, lactate oxidase and alcohol

1254   dehydrogenase, respectively.[184] Another strategy, which is conceptually similar to an ELISA, is

1255   to introduce an enzyme as a label in an affinity assay (*e.g.*, immunoassay assay, hybridization

1256   assay) that converts a coreactant to glucose for measurement. For example, the enzymatic

1257   conversion of sucrose to glucose by invertase has been used for the detection of cancer

1258   biomarkers,[190-193] nucleic acids,[194-196] small molecules,[197] ions,[198] and bacteria[199] or their

1259 biomarkers.[197] Other non-glucose assays with glucose meters have used glucoamylase for the

1260 conversion of amylopectin or amylose to glucose.[200, 201] Related strategies include the use of

1261 glucose derivatives as substrates for detecting the enzymatic activity of proteases, esterases,

1262 phosphatases, and glycosidases,[202] and monitoring the consumption of glucose by bacteria in

1263 growth media.[203]

1264

1265 **4.3 Prospective Assays with NPs**

1266 To date, the use of NPs in electrochemical POC/PON diagnostics and assays has been very

1267 limited. Of the many roles that NPs could potentially play in electrochemical assays, three roles

1268 standout as the most likely in the near future: (i) NPs as carriers for enzymes; (ii) NPs as labels

1269 for anodic stripping voltammetry (ASV); and (iii) NP-modified electrodes. The platforms for

1270 these assays may be off-the-shelf glucose meters or peripheral cell phone/smartphone

1271 attachments.

1272

1273 The use of NPs as carriers for optical contrast reagents was described in Section 3. This strategy

1274 can be adapted to affinity assays with glucose meters by modifying NPs with an oxidase enzyme,

1275 invertase, or glucoamylase. An example of the latter was reported by Fu *et al.* for the detection of

1276 neuron-specific enolase.[200] The format was an ELISA where Au NPs were modified with a

1277 reporter antibody and multiple glucoamylase enzymes for turnover of amylopectin to glucose,

1278 which was then measured with a glucose meter (Figure 17A). Analogous to the NP carrier

1279 strategy for optical readout, this strategy is expected to provide greater sensitivity by associating

1280 more enzymes with a single binding event. It is thus well-suited to increasing the sensitivity of

1281 assays with a glucose meter as the readout platform, as well as assays with a cell phone readout

1282 platform, for which a peripheral attachment has recently been developed for electrochemical

1283 ELISA assays (Figure 17B).[204]

1284

1285
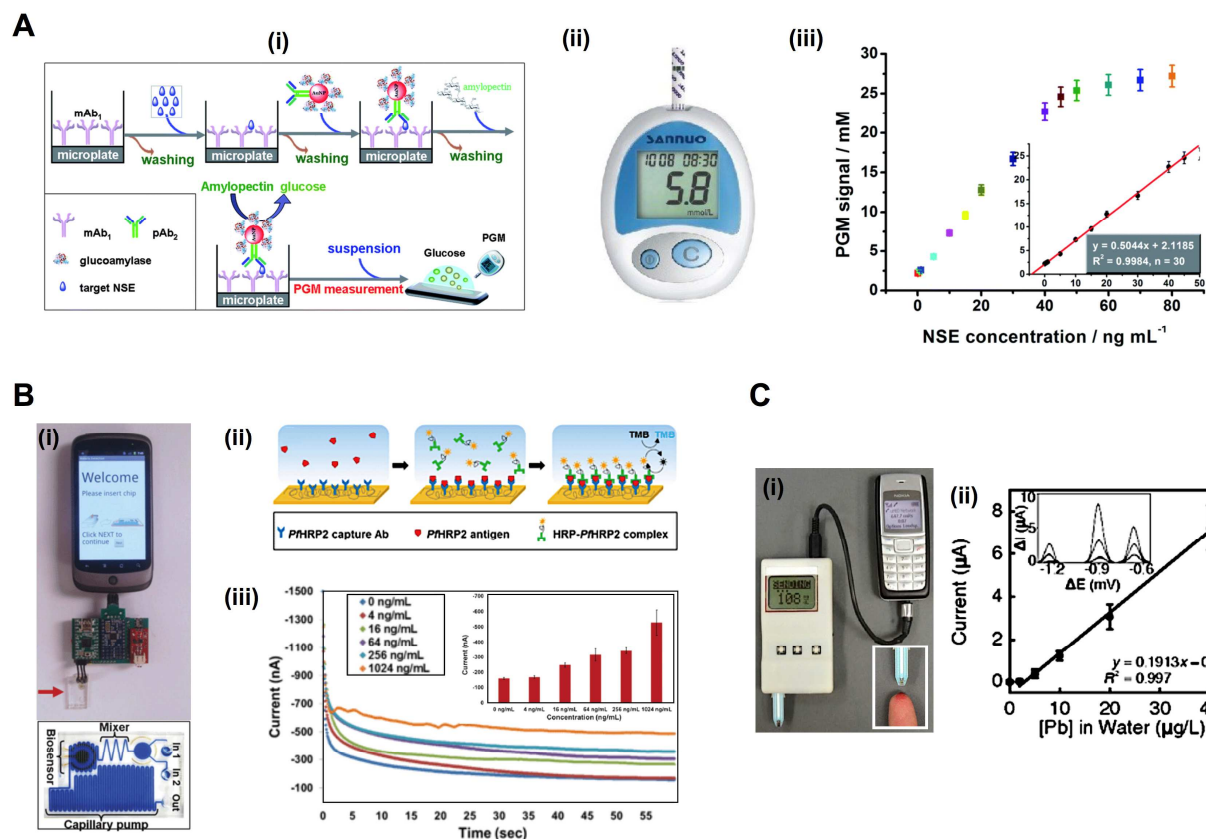
Figure 17. (A) ELISA-readout with a glucose meter: (i) design of an assay for neuron-specific enolase that achieves enzymatic amplification with turnover of amylopectin to glucose by glucoamylase; (ii) the commercial glucose meter used for assays; (iii) calibration curve for detection of neuron-specific enolase. Adapted with permission from ref.[200] **(B)** Mobile phone attachment for an electrochemical ELISA on a microfluidic chip: (i) photograph of the phone, attachment and microfluidic chip; (ii) design of an ELISA for *Plasmodium falciparum* histidine-rich protein 2 (*Pf*HRP2); (iii) chronoamperometric response to different concentrations of *Pf*HRP2 in human serum. The inset shows average current over the final 15 s of measurements. Adapted from ref.[204] with permission from The Royal Society of Chemistry. **(C)** Stripping voltammetry with a cell phone: (i) photograph of universal mobile electrochemical detector (uMED) attachment for a cell phone that is capable of electrochemical measurements; (ii) calibration plot for the detection of Pb ions using square wave anodic stripping voltammetry. The inset shows square wave voltammograms for Zn, Cd, and Pb ions (left to right). Reprinted with permission from ref.[205] Copyright 2014 the original authors.

It was recognized very early that metal NPs and some semiconductor NPs (*e.g.*, Au NPs, QDs), because they comprise many hundreds to many millions of metal atoms depending on their size, represent sensitive labels for affinity assays based on ASV.[206] In these assays, after binding and washing steps, NPs are dissolved through chemical means and the resulting ions measured by ASV. A peripheral low-cost ($25) potentiostat attachment for cell phones (Figure 17C) that is capable of ASV analysis of metal ions was recently reported,[205] and this technology would

1307 support the use of NPs as labels for affinity-based electrochemical POC assays (although the NP

1308 dissolution step may not necessarily be amenable to POC settings).

1309

1310 Another means of incorporating NPs into electrochemical POC/PON assays may be NP-

1311 modified electrodes, which have different behaviour than unmodified macroelectrodes.[207] For

1312 many POC/PON applications, paper test strips are envisioned, and screen printed electrodes have

1313 been widely used in this context.[22, 208] NPs of interest for the modification of electrodes

1314 (including screen-printed electrodes[209]) are Au and other precious metal NPs,[5] graphene and

1315 reduced graphene oxide,[210] and carbon nanotubes,[211] among other materials.[212] NP-modified

1316 electrodes have been shown to have electrocatalytic activity and facilitate direct electron transfer

1317 between electrodes and biomolecules (*e.g.*, metalloproteins), both of which are advantageous for

1318 sensing applications.[5, 210, 213] NP-modified screen-printed electrodes on paper substrates are thus

1319 likely to be investigated for electrochemical POC/PON diagnostics and assays in the near future.

1320

1321

1322 ## 5. Conclusions and Outlook

1323

1324 There is an undeniable need for POC diagnostic tests and assays that can address serious

1325 challenges in health care, both in the developed world and the developing world, as well as a

1326 parallel need for PON diagnostics in other sectors. Advances in these POC/PON diagnostics

1327 have the potential to significantly improve quality of life and drive economic gain; accordingly,

1328 research in these areas is very active and growing. The application of NPs and their unique size-

1329 dependent properties to problems of biomedical concern is also an expanding and extremely

1330 active area of research, and the convergence of this "bio-nano" research with POC/PON

1331 diagnostic research offers many exciting opportunities. In particular, the properties of NPs can

1332 enable, enhance and make easier the readout of POC/PON diagnostic results with consumer

1333 electronic devices such as cell phones and smartphones, wearable technology, scanners, disc

1334 players/optical drives, and personal blood glucose meters. The concept of using these devices is

1335 an evolution of the idea behind strip readers, which have had clinical and field success, but with

1336 the added and non-trivial benefits of mass-production and ubiquity in society.

1337

1338　From the perspective of NPs, there is still much work to be done toward POC/PON diagnostics

1339　with consumer electronic devices. Most of the work to date has exploited the optoelectronic

1340　components of consumer devices, with promising outcomes. Analytical performance can often

1341　satisfy clinical requirements and is often comparable to that with laboratory instruments that are

1342　much more expensive, non-portable, and require special training to operate. This success is, in

1343　part, a credit to the quality of the optoelectronic components in many consumer devices, but is

1344　equally (if not more so) a credit to the physical and optical properties of several NP materials.

1345　Au NPs are already widely commercialized as contrast reagents for qualitative LFAs, and

1346　readout of their intense red colour with consumer electronic devices such as smartphones, cell

1347　phones, and scanners can offer quantitation with good sensitivity. The brightness, spectrally

1348　broad absorption and narrow emission of QDs makes them an ideal material for developing

1349　sensitive, ratiometric and multiplexed fluorescence assays with smartphone readout. The

1350　upconversion luminescence and time-gating possible with UCNPs and NP-carriers of lanthanide

1351　complexes, respectively, may be able to permit direct analysis of complex sample matrices (*e.g.,*

1352　strongly coloured, autofluorescent, high concentration of particulates) that would otherwise

1353　require preparatory steps, potentially reducing the time, infrastructure and training required for

1354　the analysis. The full range of ways in which the properties of various NPs can interface with the

1355　capabilities of both consumer electronic devices and supporting technologies for POC/PON

1356　diagnostics (*e.g.*, microfluidic chips,[26, 214] paper analytical devices[20, 215]) remains to be

1357　determined. Many assay formats and optically-active NPs remain to be evaluated in this context,

1358　and the potential role of NPs in electrochemical POC/PON diagnostics is relatively unexplored

1359　when compared to optical methods. A question that will need to be addressed with the continued

1360　development of both optical and electrochemical diagnostics is the long-term storage and

1361　stability of each type of NP and their bioconjugates. Au NPs have been successful in this regard

1362　and most other NPs discussed in this review are expected to be similarly robust. The storage

1363　strategies currently used for Au NP-LFIAs will likely have some applicability with other NP

1364　materials and assays formats.

1365

1366　Current trends suggest that smartphones are well-positioned to someday become the foremost

1367　personal health care device in developed countries. These devices are exceedingly popular in

1368　younger demographics, and can function as an all-in-one tool for measurement, processing and

1369 communication of results—the latter potentially including cloud-based consultation with medical

1370 professionals. Cell phones could serve a similar role in developing countries. NPs are being

1371 recognized and demonstrated as important components for developing such POC/PON assays

1372 and diagnostic technology. Readout platforms that can be anticipated to incorporate NPs include

1373 smartphone-only platforms (no other components required; *e.g.*, LFAs with Au NPs); platforms

1374 with a smartphone and smartphone-controlled attachment (*e.g.*, dark box with an excitation light

1375 source for assays with QDs or UCNPs); and platforms based on peripheral devices that are

1376 controlled and powered by smartphones (*e.g.*, electrochemical assays). A long road lies ahead, as

1377 many of the examples discussed in this review are not yet at the point of commercialization or

1378 even clinical validation, but this road is paved in gold, semiconductors, carbon, lanthanides and

1379 other NP materials with exciting properties. The development of POC/PON diagnostics with

1380 consumer electronic devices and NPs represents a confluence of products and knowledge from a

1381 multitude of areas of science, from chemistry to electrical engineering to health and all areas in

1382 between. It promises to be an increasingly active area of research for the foreseeable future and

1383 advances in this area have the potential to have a profoundly positive impact on global health,

1384 wellness and quality of life.

1385

1386 **Disclaimer.** The brands and models of commercial devices noted or shown in this review are for

1387 informational and illustrative purposes only. No endorsements are intended.

1388

1395

1396

1397

1398 **References**
1399

1400 1.   S. Vashist, O. Mudanyali, E. M. Schneider, R. Zengerle and A. Ozcan, *Anal. Bioanal.*
1401   *Chem.*, 2014, **406**, 3263-3277.

1402 2.   M. U. Ahmed, I. Saaem, P. C. Wu and A. S. Brown, *Crit. Rev. Biotechnol.*, 2014, **34**,
1403   180-196.

1404 3.   E. Boisselier and D. Astruc, *Chem. Soc. Rev.*, 2009, **38**, 1759-1782.

1405 4.   E. C. Dreaden, A. M. Alkilany, X. Huang, C. J. Murphy and M. A. El-Sayed, *Chem. Soc.*
1406   *Rev.*, 2012, **41**, 2740-2779.

1407 5.   K. Saha, S. S. Agasti, C. Kim, X. Li and V. M. Rotello, *Chem. Rev.*, 2012, **112**, 2739-
1408   2779.

1409 6.   H. Mattoussi, G. Palui and H. B. Na, *Adv. Drug Deliv. Rev.*, 2012, **64**, 138-166.

1410 7.   E. Petryayeva, W. R. Algar and I. L. Medintz, *Appl. Spectrosc.*, 2013, **67**, 215-252.

1411 8.   C. E. Probst, P. Zrazhevskiy, V. Bagalkot and X. Gao, *Adv. Drug Deliv. Rev.*, 2013, **65**,
1412   703-718.

1413 9.   T. L. Doane and C. Burda, *Chem. Soc. Rev.*, 2012, **41**, 2885-2911.

1414 10.   F. Wang and X. G. Liu, *Chem. Soc. Rev.*, 2009, **38**, 976-989.

1415 11.   M. Haase and H. Schafer, *Angew. Chem. Int. Ed.*, 2011, **50**, 5808-5829.

1416 12.   G. Y. Chen, H. L. Qiu, P. N. Prasad and X. Y. Chen, *Chem. Rev.*, 2014, **114**, 5161-5214.

1417 13.   M. V. DaCosta, S. Doughan, Y. Han and U. J. Krull, *Anal. Chim. Acta.*, 2014, **832**, 1-33.

1418 14.   Y. Song, Y.-Y. Huang, X. Liu, X. Zhang, M. Ferrari and L. Qin, *Trends Biotechnol.*,
1419   2014, **32**, 132-139.

1420 15.   P. B. Luppa, C. Müller, A. Schlichtiger and H. Schlebusch, *TrAC, Trends Anal. Chem.*,
1421   2011, **30**, 887-898.

1422 16.   O. Clerc and G. Greub, *Clin. Microbiol. Infec.*, 2010, **16**, 1054-1061.

1423 17.   M. L. Gulley and D. R. Morgan, *J. Mol. Diagn.*, 2014, **16**, 601-611.

1424 18.   L. Anfossi, C. Baggiani, C. Giovannoli, G. D'Arco and G. Giraudi, *Anal. Bioanal.*
1425   *Chem.*, 2013, **405**, 467-480.

1426 19.   J. Hu, S. Wang, L. Wang, F. Li, B. Pingguan-Murphy, T. J. Lu and F. Xu, *Biosens.*
1427   *Bioelectron.*, 2014, **54**, 585-597.

1428 20.   A. K. Yetisen, M. S. Akram and C. R. Lowe, *Lab Chip*, 2013, **13**, 2210-2251.

1429 21.   R. Pelton, *TrAC, Trends Anal. Chem.*, 2009, **28**, 925-942.

1430 22.   B. Liu, D. Du, X. Hua, X. Y. Yu and Y. Lin, *Electroanalysis*, 2014, **26**, 1214-1223.

1431 23.   S. Byrnes, G. Thiessen and E. Fu, *Bioanalysis*, 2013, **5**, 2821-2836.

1432 24.   G. Posthuma-Trumpie, J. Korf and A. van Amerongen, *Anal. Bioanal. Chem.*, 2009, **393**,
1433   569-582.

1434	25.	D. Mark, S. Haeberle, G. Roth, F. von Stetten and R. Zengerle, *Chem. Soc. Rev.*, 2010,
1435		**39**, 1153-1182.
1436	26.	C. D. Chin, V. Linder and S. K. Sia, *Lab Chip*, 2012, **12**, 2118-2134.
1437	27.	A. C. Ng, U. Uddayasankar and A. Wheeler, *Anal. Bioanal. Chem.*, 2010, **397**, 991-1007.
1438	28.	Z. Gorocs and A. Ozcan, *Lab Chip*, 2014, **14**, 3248-3257.
1439	29.	H.-Z. Yu, Y. Li and L. M. L. Ou, *Acc. Chem. Res.*, 2012, **46**, 258-268.
1440	30.	S. Morais, L. Tortajada-Genaro and Á. Maquieira, *Expert Rev. Mol. Diagn.*, 2014, **14**,
1441		773-775.
1442	31.	P. Preechaburana, A. Suska and D. Filippini, *Trends Biotechnol.*, 2014, **32**, 351-355.
1443	32.	D. Erickson, D. O'Dell, L. Jiang, V. Oncescu, A. Gumus, S. Lee, M. Mancuso and S.
1444		Mehta, *Lab Chip*, 2014, **14**, 3159-3164.
1445	33.	X. Liu, T. Y. Lin and P. Lillehoj, *Ann. Biomed. Eng.*, 2014, 1-13.
1446	34.	I. Y. Goryacheva, P. Lenain and S. De Saeger, *TrAC, Trends Anal. Chem.*, 2013, **46**, 30-
1447		43.
1448	35.	J. Sun, Y. Xianyu and X. Jiang, *Chem. Soc. Rev.*, 2014, **43**, 6239-6253.
1449	36.	P. Yager, G. J. Domingo and J. Gerdes, *Annu. Rev. Biomed. Eng.*, 2008, **10**, 107-144.
1450	37.	A. W. Martinez, S. T. Phillips, G. M. Whitesides and E. Carrilho, *Anal. Chem.*, 2009, **82**,
1451		3-10.
1452	38.	G. Wu and M. H. Zaman, *Bulletin of the World Health Organization*, 2012, **90**, 914-920.
1453		http://www.who.int/bulletin/volumes/90/12/12-102780/en/.
1454	39.	The World Bank, "Data: Health expenditure, public (% of GDP)."
1455		http://data.worldbank.org/indicator/SH.XPD.PUBL.ZS, Accessed November 6, 2014.
1456	40.	Standard & Poor's, "Mounting Medical Care Spending Could Be Harmful to The G-20's
1457		Credit Health."
1458		http://www.standardandpoors.com/ratings/articles/en/eu/?articleType=HTML&assetID=
1459		%201245328578642. Accessed November 10, 2014.
1460	41.	Health Canada, "Canada Health Act Annual Report 2010-2011." http://www.hc-
1461		sc.gc.ca/hcs-sss/pubs/cha-lcs/2011-cha-lcs-ar-ra/index-eng.php#nu, Accessed November
1462		10, 2014.
1463	42.	Centers for Disease Control and Prevention, "Cholera - *Vibrio cholerae* infection."
1464		http://www.cdc.gov/cholera/general/, Accessed November 10, 2014.
1465	43.	J. Cameron, P. Jagals, P. R. Hunter, S. Pedley and K. Pond, *Sci. Total Environ.*, 2011,
1466		**410–411**, 8-15.
1467	44.	The United Nations Children's Fund (UNICEF)/World Health Organization (WHO),
1468		2009, "Diarrhoea: Why Children Are Still Dying and What Can Be Done."
1469		http://whqlibdoc.who.int/publications/2009/9789241598415_eng.pdf, Accessed
1470		November 16, 2014.

1471   45.   E. Corcoran, C. Nellemann, E. Baker, R. Bos, D. Osborn and H. Savelli (eds). 2010.
1472   "Sick Water? The central role of waste-water management in sustainable development."
1473   A rapid response assessment. United Nations Environment Programme, UN-HABITAT,
1474   GRID-Arendal. http://www.unep.org/pdf/SickWater_screen.pdf.

1475   46.   G. Whitesides, "A lab the size of a postage stamp." TEDxBoston July 2009.
1476   http://www.ted.com/talks/george_whitesides_a_lab_the_size_of_a_postage_stamp.

1477   47.   J. Durner, *Angew. Chem. Int. Ed.*, 2010, **49**, 1026-1051.

1478   48.   RCSB Protein Data Bank. http://www.rcsb.org/pdb/home/home.do, Accessed November
1479   8, 2014.

1480   49.   Proteomics Database. http://www.proteomicsdb.org, Accessed November 8, 2014.

1481   50.   M. Wilhelm, J. Schlegl, H. Hahne, A. M. Gholami, M. Lieberenz, M. M. Savitski, E.
1482   Ziegler, L. Butzmann, S. Gessulat, H. Marx, T. Mathieson, S. Lemeer, K. Schnatbaum,
1483   U. Reimer, H. Wenschuh, M. Mollenhauer, J. Slotta-Huspenina, J.-H. Boese, M.
1484   Bantscheff, A. Gerstmair, F. Faerber and B. Kuster, *Nature*, 2014, **509**, 582-587.

1485   51.   M. S. Kim, S. M. Pinto, D. Getnet, R. S. Nirujogi, S. S. Manda, R. Chaerkady, A. K.
1486   Madugundu, D. S. Kelkar, R. Isserlin, S. Jain, J. K. Thomas, B. Muthusamy, P. Leal-
1487   Rojas, P. Kumar, N. A. Sahasrabuddhe, L. Balakrishnan, J. Advani, B. George, S.
1488   Renuse, L. D. N. Selvan, A. H. Patil, V. Nanjappa, A. Radhakrishnan, S. Prasad, T.
1489   Subbannayya, R. Raju, M. Kumar, S. K. Sreenivasamurthy, A. Marimuthu, G. J. Sathe, S.
1490   Chavan, K. K. Datta, Y. Subbannayya, A. Sahu, S. D. Yelamanchi, S. Jayaram, P.
1491   Rajagopalan, J. Sharma, K. R. Murthy, N. Syed, R. Goel, A. A. Khan, S. Ahmad, G. Dey,
1492   K. Mudgal, A. Chatterjee, T.-C. Huang, J. Zhong, X. Wu, P. G. Shaw, D. Freed, M. S.
1493   Zahari, K. K. Mukherjee, S. Shankar, A. Mahadevan, H. Lam, C. J. Mitchell, S. K.
1494   Shankar, P. Satishchandra, J. T. Schroeder, R. Sirdeshmukh, A. Maitra, S. D. Leach, C.
1495   G. Drake, M. K. Halushka, T. S. K. Prasad, R. H. Hruban, C. L. Kerr, G. D. Bader, C. A.
1496   Iacobuzio-Donahue, H. Gowda and A. Pandey, *Nature*, 2014, **509**, 575-581.

1497   52.   Human Proteome Map. http://www.humanproteomemap.org, Accessed November 16,
1498   2014.

1499   53.   A. D. Keefe, S. Pai and A. Ellington, *Nature Reviews Drug Discovery*, 2010, **9**, 537-550.

1500   54.   S. D. Jayasena, *Clinical Chemistry*, 1999, **45**, 1628-1650.

1501   55.   National Center for Biotechnology Information (NCBI), Genome Database.
1502   http://www.ncbi.nlm.nih.gov/genome, Accessed October 29, 2014.

1503   56.   I. Ezkurdia, D. Juan, J. M. Rodriguez, A. Frankish, M. Diekhans, J. Harrow, J. Vazquez,
1504   A. Valencia and M. L. Tress, *Human Molecular Genetics*, 2014, **23**, 5866-5878.

1505   57.   F. M. Walker, K. M. Ahmad, M. Eisenstein and H. T. Soh, *Anal. Chem.*, 2014, **86**, 9236-
1506   9241.

1507   58.   L. Yan, J. Zhou, Y. Zheng, A. S. Gamson, B. T. Roembke, S. Nakayama and H. O.
1508   Sintim, *Mol. BioSyst.*, 2014, **10**, 970-1003.

1509   59.   D. S. Wishart, T. Jewison, A. C. Guo, M. Wilson, C. Knox, Y. Liu, Y. Djoumbou, R.
1510   Mandal, F. Aziat, E. Dong, S. Bouatra, I. Sinelnikov, D. Arndt, J. Xia, P. Liu, F. Yallou,

1511   T. Bjorndahl, R. Perez-Pineiro, R. Eisner, F. Allen, V. Neveu, R. Greiner and A. Scalbert,
1512   *Nucleic Acids Res.*, 2013, **41**, D801-D807.

1513 60. The Human Metabolome Database. http://www.hmdb.ca, Accessed October 15, 2014.

1514 61. D. Mabey, R. W. Peeling, A. Ustianowski and M. D. Perkins, *Nat Rev Micro*, 2004, **2**,
1515   231-240.

1516 62. British Broadcasting Corporation, BBC News: Africa, "Ebola: Mapping the outbreak."
1517   http://www.bbc.com/news/world-africa-28755033, Accessed November 17, 2014.

1518 63. Canada Broadcasting Corporation, CBC News: Canada, "Inside Walkerton: Canada's
1519   worst-ever E. coli contamination." http://www.cbc.ca/news/canada/inside-walkerton-
1520   canada-s-worst-ever-e-coli-contamination-1.887200, Accessed October 26, 2014.

1521 64. British Broadcasting Corporation, BBC News: Europe, "Denmark links 12 listeria deaths
1522   to pork sausage." http://www.bbc.com/news/world-europe-28761463, Accessed October
1523   26, 2014.

1524 65. O. A. Oyarzabal and S. Backert, *Microbial Food Safety: An Introduction*, Springer, 2011.

1525 66. U.S. Department of Health and Human Services, Food and Drug Administration, Center
1526   for Food Safety and Applied Nutrition. *Fish and Fishery Products Hazards and Controls*
1527   *Guidance.* 2011. 4th Edition. Chapter 9. Available online:
1528   http://www.fda.gov/downloads/Food/GuidanceRegulation/UCM252404.pdf.

1529 67. M. R. Monteiro, A. R. P. Ambrozin, L. M. Lião and A. G. Ferreira, *Talanta*, 2008, **77**,
1530   593-605.

1531 68. S. K. Hoekman, A. Broch, C. Robbins, E. Ceniceros and M. Natarajan, *Renew. Sust.*
1532   *Energ. Rev.*, 2012, **16**, 143-169.

1533 69. Z. Liron, A. Bromberg and M. Fisher, *Novel Approaches in Biosensors and Rapid*
1534   *Diagnostic Assays*, Springer US, 2001.

1535 70. B. Ngom, Y. C. Guo, X. L. Wang and D. R. Bi, *Anal. Bioanal. Chem.*, 2010, **397**, 1113-
1536   1135.

1537 71. R. Wong and H. Tse, *Lateral Flow Immunoassay*, Humana, 2008.

1538 72. A. Dugan, Gallup Inc., "Americans' Tech Tastes Change with Times."
1539   http://www.gallup.com/poll/166745/americans-tech-tastes-change-times.aspx, Accessed
1540   November 15, 2014.

1541 73. The World Bank. "2012 Information and Communications for Development: Maximizing
1542   Mobile,"
1543   http://siteresources.worldbank.org/EXTINFORMATIONANDCOMMUNICATIONAND
1544   TECHNOLOGIES/Resources/IC4D-2012-Report.pdf, Accessed November 20, 2014.

1545 74. P. Ha, "All-TIME 100 Gadgets," Time Magazine, October 25, 2010.
1546   http://content.time.com/time/specials/packages/article/0,28804,2023689_2023708_20236
1547   56,00.html

1548 75. International Telecommunications Union, "The World in 2014: ICT Facts and Figures."
1549   http://www.itu.int/en/ITU-D/Statistics/Documents/facts/ICTFactsFigures2014-e.pdf,
1550   Accessed November 10, 2014.

| 1551 | 76. | M. Auffan, J. Rose, J.-Y. Bottero, G. V. Lowry, J.-P. Jolivet and M. R. Wiesner, *Nat.* |
| 1552 | | *Nanotechnol.*, 2009, **4**, 634-641. |

1553   77.   E. Petryayeva and U. J. Krull, *Anal. Chim. Acta.*, 2011, **706**, 8-24.

1554   78.   T. A. Taton, C. A. Mirkin and R. L. Letsinger, *Science*, 2000, **289**, 1757-1760.

1555   79.   G. Posthuma-Trumpie, J. Wichers, M. Koets, L. J. M. Berendsen and A. van Amerongen,
1556   *Anal. Bioanal. Chem.*, 2012, **402**, 593-600.

1557   80.   Z. Li, J. C. Barnes, A. Bosoy, J. F. Stoddart and J. I. Zink, *Chem. Soc. Rev.*, 2012, **41**,
1558   2590-2605.

1559   81.   M. Montalti, L. Prodi, E. Rampazzo and N. Zaccheroni, *Chem. Soc. Rev.*, 2014, **43**, 4243-
1560   4268.

1561   82.   A. Burns, H. Ow and U. Wiesner, *Chem. Soc. Rev.*, 2006, **35**, 1028-1042.

1562   83.   M. Elsabahy and K. L. Wooley, *Chem. Soc. Rev.*, 2012, **41**, 2545-2561.

1563   84.   R. Tong, L. Tang, L. Ma, C. Tu, R. Baumgartner and J. Cheng, *Chem. Soc. Rev.*, 2014,
1564   **43**, 6982-7012.

1565   85.   I. Yildiz, S. Shukla and N. F. Steinmetz, *Curr. Opin. Biotechnol.*, 2011, **22**, 901-908.

1566   86.   M. Fischlechner and E. Donath, *Angew. Chem. Int. Ed.*, 2007, **46**, 3184-3193.

1567   87.   W. R. Algar, K. Susumu, J. B. Delehanty and I. L. Medintz, *Anal. Chem.*, 2011, **83**,
1568   8826-8837.

1569   88.   F. Wang and X. Liu, *J. Am. Chem. Soc.*, 2008, **130**, 5642-5643.

1570   89.   C. B. Jacobs, M. J. Peairs and B. J. Venton, *Anal. Chim. Acta.*, 2010, **662**, 105-127.

1571   90.   M. F. L. De Volder, S. H. Tawfick, R. H. Baughman and A. J. Hart, *Science*, 2013, **339**,
1572   535-539.

1573   91.   Y. W. Zhu, S. Murali, W. W. Cai, X. S. Li, J. W. Suk, J. R. Potts and R. S. Ruoff, *Adv.*
1574   *Mater.*, 2010, **22**, 3906-3924.

1575   92.   K. P. Loh, Q. L. Bao, G. Eda and M. Chhowalla, *Nat. Chem.*, 2010, **2**, 1015-1024.

1576   93.   S. N. Baker and G. A. Baker, *Angew. Chem. Int. Ed.*, 2010, **49**, 6726-6744.

1577   94.   J. H. Shen, Y. H. Zhu, X. L. Yang and C. Z. Li, *Chem. Commun.*, 2012, **48**, 3686-3699.

1578   95.   V. N. Mochalin, O. Shenderova, D. Ho and Y. Gogotsi, *Nat. Nanotechnol.*, 2012, **7**, 11-
1579   23.

1580   96.   R. Schirhagl, K. Chang, M. Loretz and C. L. Degen, *Annu. Rev. Phys. Chem.*, 2014, **65**,
1581   83-105.

1582   97.   C. Wu and D. T. Chiu, *Angew. Chem. Int. Ed.*, 2013, 52, 3086-3109.

1583   98.   K. E. Sapsford, W. R. Algar, L. Berti, K. Boeneman-Gemmill, B. J. Casey, E. Oh, M. H.
1584   Stewart and I. L. Medintz, *Chem. Rev.*, 2013, 113, 1904-2074.

1585   99.   K. E. Sapsford, K. M. Tyner, B. J. Dair, J. R. Deschamps and I. L. Medintz, *Anal. Chem.*,
1586   2011, 83, 4453-4488.

1587   100.   S. Feng, R. Caire, B. Cortazar, M. Turan, A. Wong and A. Ozcan, *ACS Nano*, 2014, **8**,
1588   3069-3079.

1589   101.   D. Durini, *High Performance Silicon Imaging: Fundamentals and Applications of CMOS*
1590   *and CCD sensors*, Elsevier Science, 2014.

1591   102.   iHealth Lab, Inc. http://www.ihealthlabs.com, Accessed October 8, 2014.

1592   103.   AliveCor, Inc. http://www.alivecor.com, Accessed October 8, 2014.

1593   104.   CellScope, Inc. http://www.cellscope.com, Accessed October 8, 2014.

1594   105.   SkinVision BV. http://www.skinvision.com, Accessed October 8, 2014.

1595   106.   J. A. Wolf, J. F. Moreau, O. Akilov and et al., *JAMA Dermatol.*, 2013, **149**, 422-426.

1596   107.   D. S. Bond, J. G. Thomas, H. A. Raynor, J. Moon, J. Sieling, J. Trautvetter, T. Leblond
1597   and R. R. Wing, *PloS One*, 2014, **9**.

1598   108.   J. I. Recio-Rodriguez, C. Martin-Cantera, N. Gonzalez-Viejo, A. Gomez-Arranz, M. S.
1599   Arietaleanizbeascoa, Y. Schmolling-Guinovart, J. A. Maderuelo-Fernandez, D. Perez-
1600   Arechaederra, E. Rodriguez-Sanchez, M. A. Gomez-Marcos, L. Garcia-Ortiz and E. Grp,
1601   *BMC Public Health*, 2014, **14**.

1602   109.   S. Wang, X. Zhao, I. Khimji, R. Akbas, W. Qiu, D. Edwards, D. W. Cramer, B. Ye and
1603   U. Demirci, *Lab Chip*, 2011, **11**, 3411-3418.

1604   110.   C. M. McGeough and S. O'Driscoll, *IEEE Trans. Biomed. Circuits Syst.*, 2013, **7**, 655-
1605   659.

1606   111.   C. López-Muedano, R. S. Kirton, K. D. Kumble and A. J. Taberner, *Talanta*, 2012, **100**,
1607   405-409.

1608   112.   C. F. Fronczek, T. S. Park, D. K. Harshman, A. M. Nicolini and J.-Y. Yoon, *RSC Adv.*,
1609   2014, **4**, 11103-11110.

1610   113.   V. Oncescu, M. Mancuso and D. Erickson, *Lab Chip*, 2014, **14**, 759-763.

1611   114.   A. F. Coskun, J. Wong, D. Khodadadi, R. Nagi, A. Tey and A. Ozcan, *Lab Chip*, 2013,
1612   **13**, 636-640.

1613   115.   N. K. Thom, G. G. Lewis, K. Yeung and S. T. Phillips, *RSC Adv.*, 2014, **4**, 1334-1340.

1614   116.   V. Oncescu, D. O'Dell and D. Erickson, *Lab Chip*, 2013, **13**, 3232-3238.

1615   117.   J. I. Hong and B.-Y. Chang, *Lab Chip*, 2014, **14**, 1725-1732.

1616   118.   T.-F. Wu, T. M. Yen, Y. Han, Y.-J. Chiu, E. Y. S. Lin and Y.-H. Lo, *Lab Chip*, 2014, **14**,
1617   3341-3348.

1618   119.   Q. Wei, H. Qi, W. Luo, D. Tseng, S. J. Ki, Z. Wan, Z. Göröcs, L. A. Bentolila, T. T. Wu,
1619   R. Sun and A. Ozcan, *ACS Nano*, 2013, **7**, 9147-9155.

1620   120.   H. Yu, Y. Tan and B. T. Cunningham, *Anal. Chem.*, 2014, **86**, 8805-8813.

1621   121.   A. Scheeline, *Appl. Spectrosc.*, 2010, **64**, 256A-268A.

1622   122.   S. Ayas, A. Cupallari, O. O. Ekiz, Y. Kaya and A. Dana, *ACS Photonics*, 2013, **1**, 17-26.

1623   123.   P. Preechaburana, M. C. Gonzalez, A. Suska and D. Filippini, *Angew. Chem. Int. Ed.*,
1624   2012, **51**, 11585-11588.

1625   124.   F. Deiss, M. E. Funes-Huacca, J. Bal, K. F. Tjhung and R. Derda, *Lab Chip*, 2014, **14**,
1626   167-171.

1627   125.   S. Lee, V. Oncescu, M. Mancuso, S. Mehta and D. Erickson, *Lab Chip*, 2014, **14**, 1437-
1628   1442.

1629   126.   Y. Lu, W. Shi, J. Qin and B. Lin, *Electrophoresis*, 2009, **30**, 579-582.

1630   127.   R. E. Luckham and J. D. Brennan, *Analyst*, 2010, **135**, 2028-2035.

1631   128.   D. H. Choi, S. K. Lee, Y. K. Oh, B. W. Bae, S. D. Lee, S. Kim, Y.-B. Shin and M.-G.
1632   Kim, *Biosens. Bioelectron.*, 2010, **25**, 1999-2002.

1633   129.   R. Y. T. Chiu, E. Jue, A. T. Yip, A. R. Berg, S. J. Wang, A. R. Kivnick, P. T. Nguyen
1634   and D. T. Kamei, *Lab Chip*, 2014, 14, 3021-3028.

1635   130.   K. E. Sapsford, D. Farrell, S. Sun, A. Rasooly, H. Mattoussi and I. L. Medintz, *Sens.*
1636   *Actuators B Chem.*, 2009, 139, 13-21.

1637   131.   H. Zhu, U. Sikora and A. Ozcan, *Analyst*, 2012, **137**, 2541-2544.

1638   132.   E. Petryayeva and W. R. Algar, *Anal. Chem.*, 2013, **85**, 8817-8825.

1639   133.   E. Petryayeva and W. R. Algar, *Anal. Chem.*, 2014, **86**, 3195-3202.

1640   134.   H. Kim, E. Petryayeva and W. R. Algar, *IEEE J. Sel. Topics Quantum Electron.*, 2014,
1641   **20**, 7300211.

1642   135.   E. Juntunen, T. Myyryläinen, T. Salminen, T. Soukka and K. Pettersson, *Anal. Biochem.*,
1643   2012, **428**, 31-38.

1644   136.   A. D. Warren, G. A. Kwong, D. K. Wood, K. Y. Lin and S. N. Bhatia, *Proc. Natl. Acad.*
1645   *Sci. U. S. A.*, 2014, **111**, 3671-3676.

1646   137.   M. M. Gong, B. D. MacDonald, T. V. Nguyen, K. Van Nguyen and D. Sinton, *Lab Chip*,
1647   2014, **14**, 957-963.

1648   138.   G. Zhou, X. Mao and D. Juncker, *Anal. Chem.*, 2012, **84**, 7736-7743.

1649   139.   L. Anfossi, M. Calderara, C. Baggiani, C. Giovannoli, E. Arletti and G. Giraudi, *Anal.*
1650   *Chim. Acta.*, 2010, **682**, 104-109.

1651   140.   L. Anfossi, G. D'Arco, M. Calderara, C. Baggiani, C. Giovannoli and G. Giraudi, *Food*
1652   *Addit. Contam. Part A*, 2011, **28**, 226-234.

1653   141.   B. A. Rohrman, V. Leautaud, E. Molyneux and R. R. Richards-Kortum, *PloS One*, 2012,
1654   **7**, e45611.

1655   142.   X. Shi, J. Wen, Y. Li, Y. Zheng, J. Zhou, X. Li and H. Z. Yu, *ACS Appl. Mater. Inter.*,
1656   2014.

1657   143.   M. Lönnberg, M. Drevin and J. Carlsson, *J. Immunol. Methods.*, 2008, **339**, 236-244.

1658   144.   M. Blažková, B. Mičková-Holubová, P. Rauch and L. Fukal, *Biosens. Bioelectron.*, 2009,
1659   **25**, 753-758.

1660   145.   M. Lönnberg and J. Carlsson, *J. Immunol. Methods.*, 2000, **246**, 25-36.

1661   146.   E. M. Linares, L. T. Kubota, J. Michaelis and S. Thalhammer, *J. Immunol. Methods.*,
1662   2012, **375**, 264-270.

1663   147.   M. Adhikari, S. Dhamane, A. E. V. Hagstrom, G. Garvey, W. H. Chen, K. Kourentzi, U.
1664   Strych and R. C. Willson, *Analyst*, 2013, **138**, 5584-5587.

1665   148.   J. S. Park, M. K. Cho, E. J. Lee, K. Y. Ahn, K. E. Lee, J. H. Jung, Y. Cho, S. S. Han, Y.
1666   K. Kim and J. Lee, *Nat. Nanotechnol.*, 2009, **4**, 259-264.

1667   149.   J. S. Erickson and F. S. Ligler, *Nature*, 2008, **456**, 178-179.

1668   150.   R. Gorkin, J. Park, J. Siegrist, M. Amasia, B. S. Lee, J.-M. Park, J. Kim, H. Kim, M.
1669   Madou and Y.-K. Cho, *Lab Chip*, 2010, **10**, 1758-1773.

1670   151.   M. Madou, J. Zoval, G. Y. Jia, H. Kido, J. Kim and N. Kim, *Annu. Rev. Biomed. Eng.*,
1671   2006, **8**, 601-628.

1672   152.   Abraxis, Inc., Piccolo Xpress. http://www.piccoloxpress.com, Accessed October 7, 2014.

1673   153.   Y. Li, Z. Wang, L. M. L. Ou and H. Z. Yu, *Anal. Chem.*, 2006, **79**, 426-433.

1674   154.   T. Arnandis-Chover, S. Morais, M. Á. González-Martínez, R. Puchades and Á.
1675   Maquieira, *Biosens. Bioelectron.*, 2014, **51**, 109-114.

1676   155.   S. Morais, J. Carrascosa, D. Mira, R. Puchades and Á. Maquieira, *Anal. Chem.*, 2007, **79**,
1677   7628-7635.

1678   156.   Y. Li, L. M. L. Ou and H. Z. Yu, *Anal. Chem.*, 2008, **80**, 8216-8223.

1679   157.   S. Morais, L. A. Tortajada-Genaro, T. Arnandis-Chover, R. Puchades and A. Maquieira,
1680   *Anal. Chem.*, 2009, **81**, 5646-5654.

1681   158.   S. Morais, J. Tamarit-López, J. Carrascosa, R. Puchades and Á. Maquieira, *Anal.*
1682   *Bioanal. Chem.*, 2008, **391**, 2837-2844.

1683   159.   L. A. Tortajada-Genaro, S. Santiago-Felipe, S. Morais, J. A. Gabaldón, R. Puchades and
1684   Á. Maquieira, *J. Agric. Food Chem.*, 2011, **60**, 36-43.

1685   160.   M. Pallapa, L. M. L. Ou, M. Parameswaran and H. Z. Yu, *Sens. Actuators B Chem.*,
1686   2010, **148**, 620-623.

1687   161.   S. Morais, J. Tamarit-Lopez, R. Puchades and A. Maquieira, *Environ. Sci. Technol.*,
1688   2010, **44**, 9024-9029.

1689   162.   H. Wang, L. M. L. Ou, Y. Suo and H.-Z. Yu, *Anal. Chem.*, 2011, **83**, 1557-1563.

1690   163.   X. Li, M. Shi, C. Cui and H.-Z. Yu, *Anal. Chem.*, 2014, **86**, 8922-8926.

1691   164.   X. Li, S. Wang, B. Ge, Z. Yao and H. Z. Yu, *Lab Chip*, 2014, **14**, 1686-1694.

1692   165.   V. K. Mokkapati, R. Sam Niedbala, K. Kardos, R. J. Perez, M. Guo, H. J. Tanke and P.
1693   L. A. M. Corstjens, *Ann. N. Y. Acad. Sci.*, 2007, **1098**, 476-485.

1694   166.   H. Xu, J. Chen, J. Birrenkott, J. X. Zhao, S. Takalkar, K. Baryeh and G. Liu, *Anal.*
1695   *Chem.*, 2014, **86**, 7351-7359.

1696   167.   X. Li, W. Li, Q. Yang, X. Gong, W. Guo, C. Dong, J. Liu, L. Xuan and J. Chang, *ACS*
1697   *Appl. Mater. Inter.*, 2014, **6**, 6406-6414.

1698   168.   L. Rivas, M. Medina-Sanchez, A. de la Escosura-Muniz and A. Merkoçi, *Lab Chip*, 2014,
1699   **14**, 4406-4414.

1700   169.   H. Xu, X. Mao, Q. Zeng, S. Wang, A.-N. Kawde and G. Liu, *Anal. Chem.*, 2008, **81**, 669-
1701   675.

1702   170.   J. Chen, S. Zhou and J. Wen, *Anal. Chem.*, 2014, **86**, 3108-3114.

1703   171.   Z. Zou, D. Du, J. Wang, J. N. Smith, C. Timchalk, Y. Li and Y. Lin, *Anal. Chem.*, 2010,
1704   **82**, 5125-5133.

1705   172.   Z. Li, Y. Wang, J. Wang, Z. Tang, J. G. Pounds and Y. Lin, *Anal. Chem.*, 2010, **82**, 7008-
1706   7014.

1707   173.   L. Wang, W. Chen, W. Ma, L. Liu, W. Ma, Y. Zhao, Y. Zhu, L. Xu, H. Kuang and C.
1708   Xu, *Chem. Commun.*, 2011, **47**, 1574-1576.

1709   174.   M. Ren, H. Xu, X. Huang, M. Kuang, Y. Xiong, H. Xu, Y. Xu, H. Chen and A. Wang,
1710   *ACS Appl. Mater. Inter.*, 2014, **6**, 14215-14222.

1711   175.   P. Zhao, Y. Wu, Y. Zhu, X. Yang, X. Jiang, J. Xiao, Y. Zhang and C. Li, *Nanoscale*,
1712   2014, **6**, 3804-3809.

1713   176.   G. J. van Dam, C. J. de Dood, M. Lewis, A. M. Deelder, L. van Lieshout, H. J. Tanke, L.
1714   H. van Rooyen and P. L. A. M. Corstjens, *Exp. Parasitol.*, 2013, **135**, 274-282.

1715   177.   K. Bobosha, E. Fat, S. J. F. van den Eeden, Y. Bekele, J. J. van der Ploeg-van Schip, C. J.
1716   de Dood, K. Dijkman, K. Franken, L. Wilson, A. Aseffa, J. S. Spencer, T. H. M.
1717   Ottenhoff, P. Corstjens and A. Geluk, *PLoS Negl. Trop. Dis.*, 2014, **8**.

1718   178.   OraSure Technologies, Inc., Press Release April 20, 2004. http://phx.corporate-
1719   ir.net/phoenix.zhtml?c=99740&p=irol-newsArticle&ID=516377, Accessed November
1720   14, 2014.

1721   179.   X. Song and M. Knotts, *Anal. Chim. Acta.*, 2008, **626**, 186-192.

1722   180.   C. Song, A. Zhi, Q. Liu, J. Yang, G. Jia, J. Shervin, L. Tang, X. Hu, R. Deng, C. Xu and
1723   G. Zhang, *Biosens. Bioelectron.*, 2013, **50**, 62-65.

1724   181.   M. D. Hughes, *J. Diabetes Sci. Technol.*, 2009, **3**, 1219-1223.

1725   182.   V. Gubala, L. F. Harris, A. J. Ricco, M. X. Tan and D. E. Williams, *Anal. Chem.*, 2012,
1726   **84**, 487-515.

1727   183.   S. Ferri, K. Kojima and K. Sode, *J. Diabetes Sci. Technol.*, 2011, **5**, 1068-1076.

1728   184.   Z. Nie, F. Deiss, X. Liu, O. Akbulut and G. M. Whitesides, *Lab Chip*, 2010, **10**, 3163-
1729   3169.

1730   185.   K. Tonyushkina and J. H. Nichols, *J. Diabetes Sci. Technol.*, 2009, **3**, 971-980.

1731   186.   J. Tran, R. Tran and J. R. White, *Clinical Diabetes*, 2012, **30**, 173-178.

1732   187.   Sanofi-Aventis Canada Inc., STARsstem, The iBGStar,
1733   http://starsystem.sanofi.ca/products/ibgstar-meter, Accessed November 16, 2014.

1734 188. International Diabetes Federation, IDF Diabetes Atlas, 6th Edition 2014 Update,
1735   http://www.idf.org/diabetesatlas, Accessed November 16, 2014.

1736 189. D. Dabelea, E. J. Mayer-Davis, S. Saydah and et al., *JAMA*, 2014, **311**, 1778-1786.

1737 190. Y. Xiang and Y. Lu, *Anal. Chem.*, 2012, **84**, 4174-4178.

1738 191. J. Su, J. Xu, Y. Chen, Y. Xiang, R. Yuan and Y. Chai, *Chem. Commun.*, 2012, **48**, 6909-
1739   6911.

1740 192. X. Zhu, H. Xu, R. Lin, G. Yang, Z. Lin and G. Chen, *Chem. Commun.*, 2014, **50**, 7897-
1741   7899.

1742 193. X. Ma, Z. Chen, J. Zhou, W. Weng, O. Zheng, Z. Lin, L. Guo, B. Qiu and G. Chen,
1743   *Biosens. Bioelectron.*, 2014, **55**, 412-416.

1744 194. X. Xue-Tao, L. Kai-Yi and Z. Jia-Ying, *Analyst*, 2014, **139**, 4982-4986.

1745 195. Q. Wang, H. Wang, X. Yang, K. Wang, F. Liu, Q. Zhao, P. Liu and R. Liu, *Chem.
1746   Commun.*, 2014, **50**, 3824-3826.

1747 196. Y. Xiang and Y. Lu, *Anal. Chem.*, 2012, **84**, 1975-1980.

1748 197. Y. Xiang and Y. Lu, *Nat. Chem.*, 2011, **3**, 697-703.

1749 198. Y. Xiang and Y. Lu, *Chem. Commun.*, 2013, **49**, 585-587.

1750 199. J. Joo, D. Kwon, H. H. Shin, K. H. Park, H. J. Cha and S. Jeon, *Sens. Actuators B Chem.*,
1751   2013, **188**, 1250-1254.

1752 200. X. Fu, X. Feng, K. Xu and R. Huang, *Anal. Methods*, 2014, **6**, 2233-2238.

1753 201. L. Yan, Z. Zhu, Y. Zou, Y. Huang, D. Liu, S. Jia, D. Xu, M. Wu, Y. Zhou, S. Zhou and
1754   C. J. Yang, *J. Am. Chem. Soc.*, 2013, **135**, 3748-3751.

1755 202. H. Mohapatra and S. T. Phillips, *Chem. Commum.*, 2013, **49**, 6134-6136.

1756 203. R. Chavali, N. S. Kumar Gunda, S. Naicker and S. K. Mitra, *Anal. Methods*, 2014, **6**,
1757   6223-6227.

1758 204. P. B. Lillehoj, M.-C. Huang, N. Truong and C.-M. Ho, *Lab Chip*, 2013, **13**, 2950-2955.

1759 205. A. Nemiroski, D. C. Christodouleas, J. W. Hennek, A. A. Kumar, E. J. Maxwell, M. T.
1760   Fernández-Abedul and G. M. Whitesides, *Proc. Natl. Acad. Sci. U. S. A.*, 2014, **111**,
1761   11984-11989.

1762 206. E. Katz, I. Willner and J. Wang, *Electroanalysis*, 2004, **16**, 19-44.

1763 207. S. R. Belding, F. W. Campbell, E. J. F. Dickinson and R. G. Compton, *Phys. Chem.
1764   Chem. Phys.*, 2010, **12**, 11208-11221.

1765 208. O. D. Renedo, M. A. Alonso-Lomillo and M. J. A. Martínez, *Talanta*, 2007, **73**, 202-219.

1766 209. Z. Taleat, A. Khoshroo and M. Mazloum-Ardakani, *Microchim Acta*, 2014, **181**, 865-
1767   891.

1768 210. M. Pumera, A. Ambrosi, A. Bonanni, E. L. K. Chng and H. L. Poh, *TrAC, Trends Anal.
1769   Chem.*, 2010, **29**, 954-965.

1770   211.   J. Wang, *Electroanalysis*, 2005, **17**, 7-14.

1771   212.   D. W. Kimmel, G. LeBlanc, M. E. Meschievitz and D. E. Cliffel, *Anal. Chem.*, 2011, **84**,
1772   685-707.

1773   213.   J. Lei and H. Ju, *Chem. Soc. Rev.*, 2012, **41**, 2122-2134.

1774   214.   C. T. Culbertson, T. G. Mickleburgh, S. A. Stewart-James, K. A. Sellens and M.
1775   Pressnall, *Anal. Chem.*, 2014, **86**, 95-118.

1776   215.   E. J. Maxwell, A. D. Mazzeo and G. M. Whitesides, *MRS Bulletin*, 2013, **38**, 309-314.
1777

1778 **Table 1.** Current and possible future NP materials for POC/PON diagnostics with consumer electronic devices and optical readout.
1779 The references cited are only those discussed in this review.

NP	Material [a]	Approx. Size Range	Optical Readout Features [b]	POC Usage	CMOS [c]	SCN	OD	SR
Au NPs	Gold	5–200 nm	High optical density; intense red colour; silver amplification	High	125-129	78, 136-142	154, 156, 157, 160-164	166, 168-170
Polymer NPs	Polystyrene	10–1000 nm	Properties of dopant/cargo molecule/NP (*e.g.*, QDs, lanthanide complexes)	High [d]	135	◆	◆	167, 174, 179
Amorphous Carbon NPs	Carbon	< 1000 nm (irregular)	High optical density	Moderate	◆	143-146	◆	◆
QDs	CdSe/ZnS CdSeS/ZnS	3–10 nm	Bright, tunable and spectrally narrow PL; spectrally broad light absorption	Moderate	131-133	--	--	167, 171-174
UCNPs	$NaYF_4$:Yb doped with Eu^{3+}, Tb^{3+}, Ho^{3+}	20–50 nm	Upconversion PL; spectrally narrow PL	Moderate	◆	--	--	175-177
Silica NPs	Silica	10–500 nm	Properties of dopant/cargo molecule/NP (*e.g.*, Au NPs, lanthanide complexes)	Low	◆	◆	◆	166, 180
Viral NPs	Protein	10–1000 nm	Properties of dopant/cargo molecule/NP	Low	◆	147	◆	◆
Carbon dots	Carbon	2–6 nm	Bright, spectrally broad PL	Future?	◆	--	--	◆
Pdots	π-conjugated polymers	5–50 nm	Bright PL from very strong light absorption; composites with other optically-active materials	Future?	◆	--	--	◆

Legend: CMOS, device with CMOS image sensor; OD, optical drive for disc player for CDs/DVDs/BRDs; SCN, scanner; SR, strip reader; , current use; ◆, possible or probable future use. **Notes:** [a] Typical materials listed. There are many possible materials for QDs and polymer NPs. [b] NPs may have properties beyond those listed here, refer to citations in Section 2.5 for detailed reviews of each material. [c] Includes cell phones, smartphones, digital cameras, wearable technology, *etc.* [d] There are many uncited examples of polymer NPs as carriers for dye molecules.

1780
1781
1782
1783

1784   Table of Contents Graphic

1785
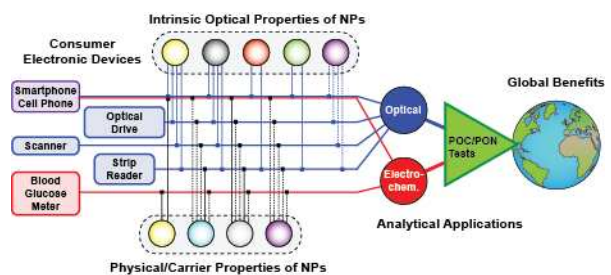
1786

1787

1788   A review of the role that nanoparticles can play in enabling and enhancing point-of-care diagnostics that utilize consumer electronic devices such

1789   as cell phones and smartphones for readout, including an overview of important concepts and examples from the literature.

1790